Differential Expression and Microsystem Physiology Reveal Predominant and Drug Reversible CFTR-Related Defects in Idiopathic Pancreatitis

Paba Edisuriya[1,2*], Pramodha Liyanage[1,2*], Jesun Lee[1,2], Anusha Jayesh Shetty[1,], Hongyu Liu[3], Nicholas Tatonetti[3,4], Danielle Hutchings[5], Alvin J. Freeman[6], Jaimie D. Nathan[6], Appakalai N. Balamurugan[7], Stephen J. Pandol[2], Anil G. Jegga[8] Anjaparavanda P. Naren[1,2,4,9#] and Kavisha Arora[1*#]

Affiliations

[1]Division of Pulmonary and Critical Care Medicine, Department of Medicine, Cedars-Sinai Medical Center, Los Angeles, CA 90048, USA

[2]Karsh Division of Gastroenterology and Hepatology, Department of Medicine, Cedars-Sinai Medical Center, Los Angeles, CA 90048, USA

[3]Biomedical Data Science Shared Resource, Cedars-Sinai Cancer, Cedars-Sinai Medical Center, Los Angeles, CA 90048, USA

[4]Department of Computational Biomedicine, Cedars-Sinai Medical Center, Los Angeles, CA 90048, USA

[5]Department of Pathology and Laboratory Medicine, Cedars-Sinai Medical Center, Los Angeles, CA 90048, USA

[6]Nationwide Children's Hospital, The Ohio State University, College of Medicine, Columbus, OH 43205, USA

[7]Wendy Novak Diabetes Institute, Norton Children's Research Institute, Norton Healthcare, Division of Endocrinology, Department of Pediatrics, Pediatric Research Institute, University of Louisville, Louisville, KY, 40202, USA

[8]Division of Biomedical Informatics, Department of Pediatrics, Cincinnati Children's Hospital Medical Center, Cincinnati, OH 45229, USA

[9]Division of Pulmonary and Critical Care Medicine, Department of Pediatrics, Cincinnati Children's Hospital Medical Center, Cincinnati, OH 45229, USA

* These authors contributed equally to this work

Anjaparavanda P. Naren and Kavisha Arora are the corresponding authors

Lead Contact: Kavisha Arora, Ph.D. Email: kavisha.arora@cshs.org

Abstract

Pancreatitis is a potentially fatal and difficult to control exocrine-tissue defect with no FDA approved therapies. Variants of a chloride/bicarbonate transporter cystic fibrosis transmembrane conductance regulator (CFTR) pose multi-fold increased risk of pancreatitis accounting for up to 40% of the patients with idiopathic pancreatitis. However, the relationship between the duct-restricted CFTR-function and total exocrine tissue defect during pancreatitis remains less known and animal models do not translate well to human disease. To overcome this challenge, we developed a robust and highly durable iPSC-derived model system of pancreatic ductal tissues from an idiopathic pancreatitis patient with a common pancreatitis-associated *CFTR* variant. In the patient line termed PANx, we found deficient CFTR function and a distinct gene expression signature for ductal tissue pancreatitis marked by aberrant mucin production, inflammatory cytokines and cystic neoplasms. By applying clinically used CFTR-modulator drug ivacaftor, we observed a remarkable restoration of deficient CFTR-mediated fluid secretion as well as upto 40% reversal of the differential gene signature for PANx including the reduction in mucinous neoplasms and immunogenic cytokines such as IL-11, CCL20 and CXCL8. We further employed a microsystem device to model hyperamylasemia, a diagnostic feature of acute pancreatitis attack, due to a ductal reaction causing acinar injury. The key mucinous signature was validated in primary pancreatitis ductal tissues with a *CFTR* variant. Overall, we unraveled new layers of CFTR-related pathology in pancreatitis to help us better understand the early course of this debilitating condition. The test methods and model systems discovered in this study will significantly expedite the discovery of diagnostic and therapeutic tools for treating idiopathic pancreatitis. For the first time, we provided molecular and physiologic evidence supporting the benefit of CFTR modulator drug ivacaftor in human CFTR-related pancreatitis.

Introduction

Acute (AP), recurrent acute (RAP), and chronic pancreatitis (CP) are potential life-threatening conditions and together remain one of the most common gastrointestinal-related cause of hospitalization in the United States[1-4]. Unabatable abdominal pain is the primary prompt for hospital admission for pancreatitis patients. The lack of any therapy in pancreatitis renders this condition extremely difficult to control. The impact of pancreatitis on patients' quality of life is substantial, as they struggle with performing daily activities and suffer from the fear of social stigma, unemployment, and depression[5,6]. Post two–three decades into the diagnosis of CP, patients have dismal survival rate of 50%[2]. The cause of AP is sudden and could be extra-pancreatic while CP is long term and associated with pancreas scarring commonly caused by alcohol toxicity, RAP episodes, or susceptibility genes[1,7]. The less common causes of pancreatitis are included in M-ANNHEIM classification system[8]. There is known to be a disease continuum among AP, RAP, and CP, with more than 10% of patients with a first episode of AP and 36% of patients with RAP developing CP[9,10].

Hereditary pancreatitis is caused by autosomal dominant mutations in the cationic trypsinogen gene (*PRSS1*) while other significant genetic susceptibilities are known including for haplotypic variants in cystic fibrosis transmembrane conductance regulator (*CFTR*) and serine protease inhibitor Kazal type 1 (*SPINK1*) genes[11,12]. Large epidemiological studies have demonstrated that carriers of *CFTR* variants are at a four-fold increased risk of developing idiopathic pancreatitis[13]. This has accounted for as many as 40% of pancreatitis patients carrying *CFTR* variants. Further *CFTR* variants increase the risk of patients undergoing total pancreatectomy with islet autotransplantation (TPIAT), which provides relief from pain but leads to long-term morbidities due to the lack of panceas-associated function[12-14]. Common pancreatitis causing insults, such as alcohol, smoking, and bile acids are also known to strongly inhibit CFTR function[11,15-17]. Thus a key factor between genetic and environmental pancreatitis etiologies is the perturbation of the CFTR protein which is largely expressed in the pancreatic ducts[11,15]. The precise mechanisms linking a lack of CFTR activity to the progression of pancreatitis including of the acinar in a genetically predisposed duct remain poorly understood. A significant limitation in the field is the absence of a relevant human-based model system to advance our understanding of pancreatitis pathophysiology. Human pancreases are scarce for research purposes, and primary tissues lack the necessary durability for long-term study[18,19]. Existing animal models, especially regarding CFTR-related pathophysiology, do not adequately replicate the characteristics and severity of human pancreatitis[20-22]. To overcome this limitation, we relied on induced pluripotent stem cells

64 (iPSCs) technology to develop a human relevant model system of the pancreatic ductal tissue to
65 study CFTR-related pancreatitis. Why study ductal tissue for pancreatitis? We know that ductal
66 passage is central to the development of pancreatitis because of the structural or physiological
67 conditions leading to ductal obstruction that causes insufficient flushing of the acini by intralobular
68 ducts culminating into auto-digestion and damage of acinar cells by hyper-concetrated enzymes
69 within the acini. Indeed, ductal ligation is a highly adopted animal model for pancreatitis[23,24].
70 Currently, there is no direct experimental evidence to support the involvement of ductal function
71 in causing exocrine damage during pancreatitis and due to delayed diagnosis early disease
72 patterns of pancreatitis in the ducts have been rarely identified. Further, it remains unknown
73 whether a deficit in CFTR function leading to a dysfunctional duct could perpetuate this cycle of
74 ductal-acinar damage, a condition that could possibly be ameliorated using CFTR-activating
75 agents. As of today many of these agents are clinically approved and highly effective in the
76 treatment of Cystic Fibrosis (CF)[25,26]. The possibility of that CFTR-agents are beneficial in the
77 treatment of pancreatitis has only been explored in a limited number of studies which are largely
78 observational[27-29]. Establishing CFTR dysfunction as a cause or contributor to idiopathic
79 pancreatitis is critical to develop care plan for these patients and understand the systemic scope
80 of their disease, and potentially allow their access to approved treatments.

81 By performing directed differentiation of induced pluripotent stem cells (iPSCs), we derived ductal
82 tissues from a patient with idiopathic RAP containing a common pancreatitis *CFTR* variant
83 V470M. This patient line also contains a mutation in CFTR modifier gene *SLC26A9*, a
84 chloride/bicarbonate exchanger and no variants for acinar cell susceptibility genes *SPINK1* and
85 *PRSS1*. Developing *de novo* ductal tissue from this line is ideal to study genetically-driven ductal
86 tissue pathology in pancreatitis to study early disease patterns without acinar involvement or overt
87 injury. Based on the comprehensive studies of iPSC-derived pancreatic cells, we identified CFTR
88 dysfunction in ductal cells from RAP patient leading to hypermucinous state characterized by
89 multifold increased expression of membrane-bound mucin MUC1 as well as secreted mucins
90 normally unexpressed by ductal cells. We additionally identified a specialized mucin expressing
91 ductal population as a characteristic of this patient line that could potentially be associated with
92 serious sequential pancreatic morbidities including the development of hypermucinous neoplasia
93 and pancreatic duct associated adenocarcinoma (PDAC). This state was remarkably reversible
94 using the CFTR potentiator, ivacaftor. Indeed, a significant proportion of the differential expression
95 state of patient cells including for the NF-κB pathway that was here identified in ductal cells, could
96 be restored to the control levels upon ivacaftor treatment suggesting a signficant drug-reversible
97 nature of pancreatitis pathology. Using a microsystem device carrying pancreatitis patient-derived

acinar cells, we established hyperviscous ductal secretion as a driver of reaction for hyperamylasemia, a feature of acute pancreatitis attack. We hypothesized that a continuum of hypermucinous and hyperviscous ductal secretion, leads to chronic acini injury and the development of pancreatitis. Overall, we discover new aspects of pancreatitis pathology and model system utilization that would accerlerate the investigation of novel molecular drivers, therapeutic targets, and diagnostics for pancreatitis.

Results

Development of iPSC-derived human model of the exocrine pancreas containing ductal tissues that closely mimics primary culture signature and growth dynamics

Pancreatic exocrine and endocrine cells originate from a common precursor, namely the pancreatic progenitor (PP) cell[30,31]. PPs acquire a tripartite state with their tip domain to give rise to the acinar lineage, while a bipotent trunk domain forms the ductal lineage together with subsequently stratifying endocrine cell types[32,33]. We followed an earlier published protocol to capture the acquisition of this central PP tripotent configuration and to further enrich differentiation into ductal lineage using ductal growth media[33]. Ductal cells were of interest to us in terms of high abundance of CFTR protein in ductal epithelial cells[34], involvement of ductal pathology, and duct-restricted *CFTR* variants in the development of RAP and CP. The iPSC-based modeling helped us overcome the limitation of obtaining very rare human pancreatitis samples, while capturing the driver genetic composition of pancreatitis patient. This model allowed us to test the specifics of ductal pathology one of which we hypothesized to be the presence of an aberrant hyper mucinous state in ductal cells based on the presence of a dominant mucus phenotype in CFTR-associated genetic disease cystic fibrosis (CF)[35] (**Figure 1a**). In this study, we compared the isolation and characteristics of primary and iPSC-derived pancreatic ductal cells from a 35-year-old female patient with idiopathic RAP (PANx line) and an age-and gender-matched control (Con). The PANx line had the following genetic mutations: In the 12 gene panel genetic testing for pancreatitis, this patient was heterozygous for a common variant of a large *CFTR* haplotype c.1408G>A (p.Val470Met, rs213950) and a silent mutation c.2562T>G (p.Thr854=, rs1042077) in *CFTR* likely in cis with both variants increasing the odds for pancreatitis when in combination with other disease causing variants. The *CFTR* variant V470M is polymorphic at the amino acid level, and variants at this locus can reduce CFTR activity by up to 60–80%[36]. This variant is also highly prevalent among general population as well as pancreatitis patients with no pathologic association in isolation and can be identified in 40–60% of individuals of all ethnicities[37]. The patient was also heterozygous for the allelic variant ‘T’ at rs7512462 in the gene *SLC26A9*, an important modifier

131 of CFTR function. Notably, this patient was homozygous for the risk factor variant in *APOB*,
132 c.13013G>A (p.Ser4338Asn, rs1042034). This common variant is associated with increased
133 serum triglyceride levels that does not cause pancreatitis in isolation but increases the risk of
134 pancreatitis.

135 To isolate primary ductal organoids (PDO), we either separated ducts from a whole pancreatic
136 tissue if available or ductal fragments from pancreatic cell remnant from TPIAT samples as
137 described earlier[18]. In **Figure 1b**, we isolated ductal tube from whole pancreatic tissue by
138 performing manual microdissection under the stereoscope, followed by EDTA treatment to
139 release stem cells for organoid growth in Matrigel to generate pancreatic ductal epithelial cells
140 (PDEC). Robust ring-like morphology could be seen that is typical of ductal organoids[18,32,38]. For
141 iPSC differentiation, we largely followed the protocol reported by Kleger's group[33] until the stage
142 of Pancreatic Trunk like Organoid (PTLO) to Pancreatic Duct like Organoid (iPDLO) differentiation
143 where we optimized a different media composition (detailed media composition and reagent
144 concentrations are described in the methods section) which yielded superior quality of ductal
145 organoids (**Figure 1c**). iPSC-differentiated cells were not characterized during the stages of
146 differentiation using any method other than being identified by the typical morphology of ductal
147 rings (**Figure 1d and 1e**) but at the end of the differentiation process (results described in **Figure**
148 **2**). At the end of the iPDLO formation and a subsequent passaging at > day 24, we were able to
149 sort the epithelial cell marker Epithelial Cell Adhesion Molecule ($EPCAM^+$) population. Nearly 99%
150 of the cells were $EPCAM^+$ in both the control and PANx lines suggesting a pure epithelilal
151 composition of the iPSC-differentiated cells (**Figure 1e**). We also compared the growth dynamics
152 of $EPCAM^+$-derived PDO of primary as well as iPSC-origin (**Figure 1f**). Although primary
153 organoids exhibited robust growth in the initial 2-4 days, the growth rate of all the organoid types
154 was on par with each other including for the PANx line over extended days of culture > 7 days.
155 However, the PANx-iPDLOs were consistently smaller in size compared to the controls (**Figure**
156 **1f**). We used these organoids to isolate single cells for further molecular and functional
157 characterization.

158 **iPSC-derived control and PANx cells expressed all key pancreatic ductal cell markers**

159 Here, we first characterized the molecular signature of control and PANx ductal cells at > Day 27
160 of iPDLO formation and post-passage two. Based on global-transcriptome sequencing, primary
161 as well as iPSC-derived ductal cells showed high expression of cytokeratin 19 (*KRT19*), E-
162 cadherin (*CDH1*), zonula occludens 1 (*ZO1*) or tight junction protein 1(*TJP1*), and adult stem cell
163 marker transcription factor SRY-Box Transcription Factor 9 (*SOX9*) and low expression of β-cell

164 enriched and ductal cell pancreatic and duodenal homeobox 1 (*PDX1*). No marker gene
165 expressions for acinar cells (amylases, *AMY*) and β-cells (insulin, *INS*) were present in the
166 differentiated cells from both lines (**Figure 2a**). These expression patterns were very similar to
167 those of the primary ductal organoids and there was no difference in the expression of these
168 markers between the control and PANx cells (**Figure 2a**). The expression of *CFTR* was also
169 confirmed along with other key transporters for bicarbonate secretion in the control and PANx
170 iPDLCs albeit at a lower level for *CFTR* compared to the primary cells (**Figure 2b**). Using single-
171 cell sequencing, we confirmed that iPSC-derived differentiated cells were homogenously ductal
172 ($KRT19^+$, $EPCAM^+$) and formed three major clusters with seven subclusters that we named ductal
173 mix (composed of mature ductal (cadherins rich), likely endocrine adjunct or transitioning to
174 endocrine based on several overlapping genes expressed in β-cells, and ductal cells undergoing
175 nuclear transformation/DNA repair), actively proliferating and of secretory/mucinous phenotypes
176 (**Figure 2c, Supplementary Figure 1a and 1b**). The presence of ductal markers corresponding
177 to ZO1, KRT19 and CFTR was confirmed at the protein level using immunofluorescence with no
178 detectable difference of expression between the control and PANx cells (**Figure 2d**).

179 **Pancreatitis associated *CFTR* variant caused reduced CFTR activity that could be restored**
180 **using CFTR-activating agents**

181 Given that our goal is to understand the ductal pathology due to CFTR-related defect as
182 anticipated for the *CFTR* variant in the PANx line, it become impertive to evaluate the function of
183 CFTR in the PANx cells and compare it with control cells. It was also crucial to conduct this
184 experiment to ensure the formation of a functional ductal epithelium from iPSC-differentiation.
185 CFTR function was evaluated using whole-cell patch clamping in single primary, control, and
186 PANx cells. Primary cells tended to have higher CFTR function than control iPDLCs, but the
187 difference was not statistically significant over the number of independent experiments that were
188 performed (**Figure 3a and 3b**). None of the single patch-clamped PANx cells demonstrated CFTR
189 function corresponding to a total current density of < 0.15 pA/pF and no detectable CFTR-
190 inhibitor-172 (CFTRinh-172) sensitive response while 70% of the control cells showed clear
191 CFTRinh-172 sensitive response upon stimulation using cyclic AMP (cAMP) or cAMP agonist
192 forskolin (FSK) with a median current density of 2.68 pA/pF (**Figure 3c-3e**). We further explored
193 the possibility that the functional consequences of the mutation may be treatable
194 with *CFTR* targeted therapies. Ivacaftor or VX-770 (Brand name: Kalydeco®) is a clinically
195 approved drug used to treat CF in individuals with specific mutations involving gating and
196 conductance defects in the CFTR protein[26]. Ivacaftor is a potentiator that directly binds to CFTR

197 and helps open the channel[39,40]. The binding site is now known based on the cryo-EM structure
198 of ivacaftor in complex with phosphorylated CFTR[41]. Ivacaftor docks into a cleft formed by
199 transmembrane (TM) helices 4, 5, and 8. The predictable binding site is at the signature hinge
200 region in TM8 of the CFTR. The extracellular region of TM 8 rotates around this hinge upon ATP
201 binding, which can be stabilized by ivacaftor. Ivacaftor is known to open even normal CFTR
202 channels and can restore sub-optimal CFTR function as well. Therefore, it can be evaluated as a
203 CFTR-activating agent without the disease pathology for CF and its benefit has been established
204 in a few CFTR-related non-CF conditions[39,40]. Unlike other CFTR activating agents, ivacaftor is a
205 specific potentiator of CFTR activity and hence more suitable agent for evaluating the benefits of
206 CFTR activation and CFTR-directed therapies in human diseases. Also, since PANx cells
207 expressed CFTR protein but showed a deficit in function, this line is suitable to test ivacaftor.
208 Consistent with our expectation, PANx cells exhibited a remarkable rescue of CFTR response to
209 VX-770 treatment in 78% of the tested cells with a median response of 2.97 pA/pF (**Figure 3c-**
210 **3e**). The functional heterogeneity of the cells for CFTR is expected in asynchronous non-clonal
211 single cell preparations, meaning that not all cells will have functional CFTR leading to a high
212 degree of variability in this assay. To overcome this limitation, we sorted to measure macroscopic
213 CFTR-inhibitor responsive short-circuit currents. These currents were stimulated using FSK
214 stimulation and calculated as *ΔIsc* for iPDLC that were cultured as monolayers on semipermeable
215 transwell supports and formed highly resistant epithelium within 7 days of culture (1500-2000
216 Ω/cm^2). We observed similar CFTR-mediated *Isc* in primary and control ductal cells at ΔIsc ± SD
217 of 4.76 ±1.32 and 4.22 ± 0.34 $\mu A/cm^2$, respectively, while PANx demonstrated significantly low
218 but positive CFTR ΔIsc ± SD 1.33 ± 0.75 $\mu A/cm^2$ (**Figure 3f and 3g**). Consistent with earlier
219 results, VX-770 significantly improved CFTR ΔIsc in PANx cells to 2.6 ± 0.9 $\mu A/cm^2$. Another
220 highly adopted method to measure CFTR-dependent function is monitoring FSK-elicited fluid
221 secretion or FSK-induced swelling (FIS) in the 3D Matrigel-embedded organoid system calculated
222 as total organoid area post-FSK stimulation[42,43]. Using FIS, we were able to recapitulate the
223 reduced function of CFTR in PANx iPDLO with an estimated 50% reduction in function and a
224 rescue of function using VX-770 (**Figure 3h and 3i**).

225 Given that CFTR is a cAMP-regulated chloride channel, there are additional FDA-approved drugs
226 that are in clinical use for various human conditions that alter cAMP signaling, including inhibitors
227 of the cAMP and cGMP degrading enzymes-phosphodiesterases (PDEs). Based on
228 transcriptomic analysis, cAMP-degrading PDEs, such as PDE4A, PDE7A, PDE8A and PDE12,
229 cGMP-degrading PDEs PDE5A, PDE6B, PDE6D and PDE9A, and dual-specificity PDEs PDE3A,
230 PDE3B and PDE10A were abundantly expressed in control and PANx iPDLCs (**Figure 3j**). The

most notable finding is the relatively high abundance of cGMP degrading enzymes-PDE5A and PDE9A. Rolipram is a selective PDE4 inhibitor that has been researched for its benefit in the treatment of Alzheimer's Disease and inflammatory respiratory conditions such as asthma[44]. Zaprinast is a precursor to the drug sildenafil (Viagra), which is a PDE-5,6,9 and 11 inhibitor and is in clinical use for the treatment of erectile dysfunction[45]. It was originally considered as a treatment for allergic asthma and cardiovascular diseases[46,47]. Cilostazol is a potent PDE3A inhibitor that is used to treat periphery artery disease via vasodilation through cAMP generation[48]. Given the abundance of select cAMP and cGMP PDEs in iPDLC, which are targets for the above-described drugs, we tested the effect of these compounds on CFTR function in the control and PANx iPDLO using FIS assay as this assay is amenable to medium throughput testing for multiple drugs. Zaprinast and cilostazol in combination with FSK generated most robust CFTR FIS response in PANx iPDLO that did not plateau after 72 h of measuring fluid secretion response vs. FSK alone (**Figure 3k**). The control iPDLO also responded positively to zaprinast and cilostazol treatment relative to the FSK treatment alone (**Figure 3k**). These data suggest that PDE inhibitors can be considered as therapeutic candidates for restoring CFTR functional defects during pancreatitis.

Ductal cells with pancreatitis exhibited a hypermucinous state and other pathological features that were reversible in the presence of ivacaftor treatment

Given that CFTR activity is directly related to the mucus phenotype in various CF organs[49], we investigated the possibility of mucus pathology in PANx cells. Based on the global transcriptomic analysis, there was a multi-fold increase in mucin levels, with a significant increase in membrane-bound mucin 1 (*MUC1*) and secreted mucin 5AC (*MUC5AC*) in PANx cells compared to the control cells (**Figure 4a**). Only majorly expressed MUCs in ductal cells were plotted. One prominent example of the mucin biosynthesis pathway is Trefoil factor 1 (*TFF1*), which is synthesized by the surface mucous cells across the gastric epithelia and is known to be co-secreted with MUC5AC to aid in the formation of mucous layer[50,51]. Both *TFF1* and *MUC5AC* were upregulated by more than 10-fold and 200-fold respectively, in PANx cells (**Figure 4a**). Galectin 3 (*LGALS3*) is another gene that was highly upregulated at > 4-fold change in PANx cells (**Figure 4a**) and plays a role in stabilizing the mucus layer by interacting with the sugar moieties on the mucins[52]. Another contributing genetic factor to the mucus phenotype was the highly upregulated expression of a protease inhibitor WAP four-disulfide core domain protein 2 (*WFDC2*) in PANx cells (**Figure 4a**) which contributes to the secretion and formation of mucus barrier and is expressed by mucous cells[53]. A significant increase in the expression of REG4 (32-fold) (**Figure**

264 **4a**) also suggested an increase in the secretory cell phenotype [54]. Our single cell analysis also
265 demonstrated enrichment for mucinous ductal cell population in PANx ductal cells marked by
266 MUC5AC, MUC5B and MUC1 within the mucinous population (**Figure 4b**). At the level of the
267 protein, there were much higher levels of secreted MUC5AC in PANx cells vs. control under
268 reducing conditions using dithiothreitol (**Figure 4c**). Importantly, the expression levels of both the
269 transcripts as well as secreted protein for MUC5AC were restored to the control values upon 24-
270 48 h treatment with VX-770 (**Figure 4a and 4c**). Using a biotinylated mucin binding probe (Mucin
271 Probe, biotin-StcE) and epithelial cell-specific stain detecting CDH1, we identified large cystic
272 structures in PANx transwell differentiated cultures that also showed larger nuclei exhibiting the
273 characteristics of mucinous neoplasms (**Figure 4d-4f, Supplementary Figure 2a**). Remarkably,
274 these structures largely resolved upon treatment with VX-770 (**Figure 4c-4f**). The PANx line
275 exhibited distinct mucous cells and membrane-bound mucins that were in complete absentia in
276 control cells and disappeared upon treatment with VX-770 (**Figure 4d and 4f**). Intraductal
277 mucinous pancreatic neoplasms are mucin-producing cystic lesions of the exocrine pancreas,
278 usually localized within the pancreatic ducts[55,56]. Dysregulated activities of
279 *KRAS*, *CDKN2A*, *TP53*, and *SMAD4* are strongly associated with the development of
280 neoplasms[57,58]. In the PANx line, tumor suppressor *TP53* expression was significantly
281 downregulated in the PANx line and was restored to the control level in the presence of VX-770,
282 whereas *KRAS*, *CDKN2A* and *SMAD4* were not altered (**Supplementary Figure 2c**).
283 Approximately 15% to 30% of ductal neoplasms may be malignant[59]. The primary marker used to
284 identify malignant mucinous pancreatic neoplasms is carcinoembryonic antigen cell adhesion
285 molecule 1/5 (CEACAM1/5) secreted into the ductal fluid[60]. Unfortunately, the patient line
286 demonstrated exceedingly high levels of *CEACAM5* at the mRNA level compared with the control
287 line suggesting likely malignancy which remain clinically undiagnosed in this patient as of now
288 (**Supplementary Figure 2b and 2c**). The *CEACAM5* levels were also restored to the normal
289 levels in the presence of VX-770. DKK1, an antagonist of Wnt/β-catenin signaling, was
290 downregulated by >4-fold in PANx cells, indicating an increased migratory effect and potential
291 role in tissue metastasis [61] and VX-770 had a marginal effect on increasing its levels
292 (**Supplementary Figure 2c and Figure 5d**). Therefore, not only the restoration of defective CFTR
293 function, but we also established the multi-layered benefits of VX-770 on pancreatitis that could
294 be due to CFTR-related primary or secondary events.

295 At the global transcriptomics level, there were a total of 940 differentially expressed genes (DEGs)
296 for PANx: 485 up and 455 downregulated genes (**Figure 5a-5b**). At log2 fold threshold of 1, 41%
297 of the differentially altered genes in PANx vs. control were affected by VX-770 treatment. We

298 labeled these as CFTR activity-responsive genes (**Figure 5b**). Among these, genes associated
299 with mucin biosynthesis (51/940 DEGs; 49/51 up and 2/51 down) and inflammation (107/940
300 DEGs) as anticipated for the PANx line were significantly affected, and this signature was notably
301 reversible in the presence of VX-770 (**Figure 5f, Supplementary Figure 3a**).

302 A general view of the pancreatitis pathology is that it is caused by a combination of auto-digestive
303 reactions due to premature activation of trypsinogen within the pancreatic acini and a parallel
304 inflammatory cascade due to the recruitment of macrophages and granulocytes both leading to
305 tissue damage[62,63]. Ductal and acinar cells themselves release several pro-inflammatory
306 cytokines, such as interleukin (IL)-1, IL-6, IL-8, IL-18, IL-33, and tumor necrosis factor (TNF)-α to
307 start a vicious process of pancreatic injury and inflammation and eventually systemic injury that
308 can lead to death[64,65]. Sustained intra-acinar activation of nuclear factor-κB (NF-κB) downstream
309 of initial injury appears to be the triggering event in the development of inflammation in chronic
310 pancreatitis[66]. Indeed, the major pathways that were upregulated in PANx cells included HIF1α
311 and NF-κB signaling which are associated with an increased production of inflammatory cytokines
312 (**Figure 5c and 5d, Supplementary Figure 3a**). Treatment with VX-770 had remarkably reverted
313 this signature in the PANx cells with several genes affected by VX-770 as mapped in the NF-κB
314 signaling network (**Figure 5e**). We also listed the key cytokines that were upregulated in the PANx
315 line (**Table 1**) many of which have already been established as pro-inflammatory and are known
316 to play a role in pancreatitis including IL-11, IL-33 and several members of the C-X-C motif
317 chemokine (CXCL) family (CX3CL1, CXCL1, CXCL12, CXCL16, CXCL5, CXCL8). Among the
318 notable pro-inflammatory cytokines, following cytokines levels were reduced by VX-770: CCL20,
319 CCL28, CXCL8 and IL-11 (**Table 2**). The PANx line showed an abundance for signature
320 corresponding to the formation of pancreatic lesions (260/940 DEGs; 140/260 up and 120/260
321 down) (**Supplementary Figure 2b**) as was morphologically and immunohistochemically captured
322 in the earlier observations. Due to the presence of APOB mutation in the PANx line, we also
323 examined pathways for lipid homeostasis in the cells (**Supplementary Figure 3b**). S4338N
324 *APOB* mutation is known to be associated with hypercholesterolemia, hypertension,
325 atherosclerosis and coronary heart disease. DGE analysis suggested that a total of 69 genes
326 were altered in the lipid biosythesis pathway (69/940 DEGs) that were affected by VX-770
327 (**Supplementary Figure 3b**). However, there was no clear indication of abberration of lipid
328 homeostasis in PANx cells based on pathway analysis.

329 We used primary ductal pancreatitis tissue obtained from TPIAT remnant samples to validate our
330 data from iPSC-derived ductal tissues regarding mucinous pathology and its association with

331 CFTR. A similar hypermucinous signature was present in ductal cells with *CFTR* variants
332 compared to those without variants and only pancreatitis-related *SPINK1* mutation (**Figure 5g**).
333 This signature was characterized by an increased transcriptional profile for several mucin genes,
334 predominantly MUC5B, and an enhanced secretory cell program regulated by TFF1 and REG4.
335 The secreted mucin score was calculated for primary and iPSC-derived ductal tissues based on
336 cumulative counts of secreted mucins (MUC2, MUC5AC, MUC5B, MUC6, MUC7, and MUC19),
337 showing an overlapping trend of enhanced mucin secretion with the iPSC-derived PANx ductal
338 cells and specific to the state of presence ot absence of a *CFTR* variant (**Figure 5h**). Therefore,
339 this data strongly supports the presence of a common hypermucinous state across CFTR-related
340 pancreatitis and demonstrates the robustness of our iPSC model system in recapitulating this
341 pathology.

342 **Modeling hyperamylasemia as a function of hyperviscous ductal fluid using a microsystem**
343 **device**

344 The loss of acinar function is a known feature of pancreatitis and could be a consequence of
345 acinar damage[67,68]. Hyperamylasemia, which is defined as elevated serum amylase levels
346 >110U/ml, is a common finding in up to 75% of cases of pancreatitis[69]. Hyperamylasemia is
347 primarily caused by damaged acini in pancreatitis[70]. Elevated serum amylase is routinely used as
348 a biomarker for acute pancreatitis attack. Elevated amylase levels have earlier been reproted to
349 be consistently associated with the presence of *CFTR* and *SPINK1* mutations[71]. There is also a
350 direct correlation between elevated amylase and low pH of the pancreatic juice[72]. Periodic Acid-
351 Schiff (PAS) staining in pancreatic tissues revealed a high secretory state in ductal epithelial cells,
352 characterized by glycoproteins, including mucins (**Figure 6a**). These glycoproteins contribute to
353 the composition of ductal secretions, which are released through a branching network of ducts
354 originating from the main duct. This network forms interlobular and intralobular duct systems that
355 extend to the terminal acinar compartments. We hypothesized that more viscous ductal fluid
356 composition due to a deficit in CFTR function causes insufficient flushing of acini and
357 accumulation of digestive enzymes, leading to acinar damage and thus increased amylase
358 accumulation or release. To artificially enhance the viscosity of ductal fluid, we used 10% glycerol
359 which is known to have no apparent impact on cell viability by itself and be often used as a
360 cryopreserving agent. We utilized a commercially available chip from Ibidi that enabled
361 communication between two chambers via a narrow channel (**Figure 6b**). We seeded primary
362 acini freshly isolated from pancreatic tissues with no apparent defects in isolated acinar activity in
363 one chamber and applied 60 µl of the apical fluid from control ductal cells differentiated on TW as

364 is or mixed with 10% glycerol while maintaining the effective composition of ductal fluid at 90%
365 under both conditions. After 24 h of incubation, we performed amylase activity assay to assess
366 acinar cell function. Acinar cells exposed to a more viscous fluid secreted ~1.5-fold higher
367 amylase compared to the ductal fluid without glycerol (**Figure 6c**). We next assessed whether
368 increased viscosity was associated with acinar cell damage. Cells exposed to viscous ductal fluid
369 exhibited ~3-fold higher LDH activity, suggesting damage (**Figure 6d**). Since glycerol can act as
370 a weak base, we checked media pH at the concetration of 10%, glycerol and it did not cause any
371 pH change in the media. These data suggest that fluid viscosity has an impact on acinar cell
372 condition, and this is a likely pathological scenario in the case of reduced CFTR activity and
373 related increase in ductal fluid viscosity during the development of pancreatitis.

374 **Discussion**

375 Pancreatitis is a debilitating condition that significantly impacts quality of life and progresses
376 rapidly due to poor prognosis and limited strategies for pain management. Pancreatitis-related
377 studies are limited because of the lack of tangible model systems that recapitulate key
378 pathological features of pancreatitis. Using iPSC-derived modeling, we were able to recapitulate
379 clear pancreatitis-related pathology in the ductal epithelium derived from a patient with idiopathic
380 pancreatitis who carried a common pancreatitis-related *CFTR* variant. Importantly and
381 surprisingly, the pancreatitis signature is inherently present in these cells without an overt injury.
382 Nearly 40% of patients with pancreatitis are known to carry various *CFTR* variants. Several
383 hurdles have been identified in the establishment of an early diagnosis as well as clear
384 pathological course for pancreatitis. First, there are several non-specific symptoms of pancreatitis
385 that overlap with other conditions[73,74]. Second, diagnostic imaging of the pancreas remains
386 inconclusive in many cases and is highly variable[75]. Third, specific biomarkers for diagnosing
387 pancreatitis in early stages of development are lacking[76]. Fourth, several genetic alterations or
388 environmental factors may be involved, leading to complex pathology, and multiple tissue systems
389 are usually impacted in the disease development. The development of human model system
390 remains central to understand the aspects of early pathogenesis of the human disease and cell-
391 type specific pathology, and to test and develop therapies. By generating pure pancreatic cell-
392 types, more complex multi-tissue systems can be evolved by precise cell-mixing to understand
393 the involvement of multiple cell-types and specific cell-cell communication in disease
394 development. We established that using an iPSC-derived model system of pancreatic ductal cells,
395 deficit in CFTR function within the ducts can drive pathology of idiopathic pancreatitis in the
396 patients with a common CFTR variant. This is a contrasting finding for the commonly held notion

397 for acini as the site for initial pancreatitis injury[63]. This finding is further supported by the data that
398 by rescuing CFTR function using FDA approved CFTR modulator ivacaftor several pancreatitis
399 associated pathological characteristics that align with the clinical features of pancreatitis could be
400 reversed. Nearly, 40% of the pancreatitis-related ductal cell genes responded to ivacaftor
401 treatment suggesting the presence of a major CFTR associated pancreatitis signature.

402 In CF, CFTR protein product is defective and associated with devastating lung infections and
403 other extra-pulmonary manifestations including pancreatic insufficiency and meconium ileus[35]. A
404 major pathological feature of CF in these organs is the development of mucus plugs and
405 hyperviscous conditions in the airway, pancreas, and gut[35,77]. A deficiency in fluid secretion alters
406 the mucus properties resulting in the failure of attachment from the mucous cells[78]. Viscosity is
407 an important parameter for fluid that is secreted into the tubular configurations of the airway,
408 pancreas, and gut for lubrication and, flow, flushing, dilution, and release of the luminal factors.
409 Fluid properties are significantly altered in CF and that was the hypothesis that we tested in this
410 pancreatitis model due to CFTR-related defect. To our surprise, the mucus defect was
411 predominantly associated with the development of pancreatic neoplasms that were
412 hypermucinous and developed in the transwell differentiated cultures of the pancreatitis line. This
413 pathological transformation is the common sequale of chronic pancreatitis. This mucinous
414 pathology is distinct from CF which is normally characterized by goblet cell hyperplasia and
415 abnormal sticky mucus[79]. We exposed normal acinar cells to a hyperviscous environment using
416 glycerol on a chamber device composed of two compartment interactions through a narrow
417 channel, we were able to model hyperamylasemia characterized by upregulated production of
418 amylase associated with acinar cell damage. The viscosity was simulated using 10% glycerol,
419 which is known to have no effect on cell viability. The acinar cells maintained in both environments
420 i.e. normal ductal fluid and ductal fluid plus glycerol did not show any apparent difference in cell
421 quality and morphology. Further, the pancreatitis cells served as the primary source for the
422 expression of CEACAMs that are used as the biomarker for pancreatic cancers[80] and this feature
423 was reversed by ivacaftor. The role of CEACAMs is suggested to be key in driving the
424 inflammatory response during pancreatitis[81].

425 Notable inflammation driving pathways that were significantly high in the PANx cells were NF-
426 κB and HIF-1 signaling[82] that are known to directly increase the production of various pro-
427 inflammatory cytokines such as TNF-α, IL1β and chemokines during pancreatitis and are also
428 known to be highly elevated in animal models of pancreatitis[83]. The HIF-1 pathway also
429 contributes to the tissue necrosis leading to pancreatic injury. Ductal cell-derived cytokines such

430 as IL-11, CCL20 and CXCL8 were highly upregulated in PANx cells and reverted to normal control
431 levels using ivacaftor (Table 2). These cytokines are known to propagate immune cell infilteration
432 and fibrosis during pancreatitis[84].

433 The question arises whether this study is useful for pancreatitis in patients with other mutation
434 types. This study highlights ductal tissue pancreatitis which is foundational for studying
435 pancreatitis in patients with various CFTR variants provided with an evidence of CFTR
436 dysfunction irrespective of the nature of mutation. We found that CFTR functional deficit is
437 associated with key pathological features of pancreatitis. The molecular and morphological
438 features observed with the PANx line overlap with clinically reported features in the general
439 population however, we revealed new layers of information such as drug-reversible disease
440 features in pancreatitis and that CFTR dysfunction in ductal tissue can drive mucinous pancreatic
441 neoplasms, inflammation, and could be associated with pancreatitis attacks. We were able to
442 validate a similar hypermucinous states in primary pancreatitis ductal tissue with a *CFTR* variant
443 which was absent in another paitent sample with no *CFTR* variant and mutation in PRSS1 gene.
444 Therefore, we expect a broad application of these findings to other pancreatitis patients even with
445 differenet set of mutations.

446 As a model system, iPDLCs exhibited long-term passaging capabilities (15-20 passages) and
447 retained their cellular, molecular, and functional characteristics, unlike primary cells, which are
448 challenging for long-term growth beyond passage 5[18,19]. iPDLCs were suitable for multiple
449 applications, including physiologic assays and expression-based analysis. This study establishes
450 a pipeline for utilizing such a model system for drug development, repurposing, and therapeutic
451 testing. There are major species-driven differences in pancreatic structure and diseases[20,85].
452 Many therapeutic agents beneficial in mouse models of pancreatitis have not been clinically
453 translated[86]. Using the human-based model system, we established that CFTR-specific agent
454 ivacaftor can reverse several pathological features of pancreatitis, including downstream
455 sequelae such as cancer. Pancreatic cancers consittute the largest risk for death among
456 pancreatitis patients. This approach could be a breakthrough treatment for patients with
457 pancreatitis as we identified hypermucinous neoplasms as reversible pathology in CFTR-related
458 pancreatitis, potentially a primary or secondary event to CFTR functional activation.

459 **Study approval**

460 This study was approved by the Cedars Sinai Medical Center Institutional Review Board study
461 titled CFTR functional studies, STUDY00001735.

Acknowledgments

This work was funded by Cedars Sinai Pilot Feasibility award to KA, Cystic fibrosis Foundation, and National Institutes of Health (NIH) awards DK080834 and P30-DK117467 to APN. We thank Dr. Maisam A. Abu-El-Haija, MD, Medical Director, Pancreas Care Center, Cincinnati Children's Hospital for providing the TPIAT samples. We thank Dr. Dhruv Sareen, Executive Director, Cedars-Sinai Biomanufacturing Center, for help generating control and patient's iPSC lines. The authors thank Ms. Bonnie Paul for assisting with coordinating patient studies following rigorous regulatory measures for human subject-based studies.

Footnotes

Conflict of interest: The authors declare that no conflict of interest exists pertinent to this manuscript.

Methods and supplementary figures and legends are included in the supplementary information.

Author contributions

The study was conceived by PE, APN and KA and supervised by APN and KA. JL conducted whole cell patch clamp experiments. PL, HL, NT and AGJ analyzed transcriptomic data. DH assisted with the analysis of mucinous pancreatic neoplasms. AF, JDN, BA and SRP reviewed and edited the manuscript and provided key clinical insights into the study. PE and KA wrote the first and several other draft manuscripts before sending a version to all authors to comment on. All authors received, commented on, and approved the submission of this manuscript.

490 **Figure legends**

491 **Figure 1. Pancreatitis model of human ductal tissue containing a common *CFTR* variant**

492 **a.** Diagrammatic representation of the events hypothesized to be related to deficit in CFTR
493 function due to the presence of CFTR variants in idiopathic pancreatitis. A lack of CFTR
494 function leads to insufficient flushing of the acini compartment causing accumulation of
495 digestive enzymes that over time lead to acinar and duct damage i.e. autoproteolysis,
496 progressive inflammation and pancreatitis. To investigate CFTR-related pathology in
497 pancreatitis, human model systems, which can be sourced from primary tissues i.e.,
498 pancreatic resections are required. Alternatively, the differentiation of iPSCs into pancreatic
499 structures such as ductal tissues is a highly feasible and readily available approach to study
500 ductal pathology including mucus related defects in pancreatitis.

501 **b.** Isolation of ducts from whole pancreatic tissue (non-pancreatitis) followed by EDTA treatment
502 to release stem cells (Day 0) to form ductal organoids that grow and show typical ring-like
503 morphology with large luminal area (Day 15).

504 **c.** Stepwise schemata of the differentiation of iPSCs into ductal progenitors and the formation of
505 pancreatic duct like organoids.

506 **d.** Bright-field images show different stages of iPSC differentiation of a control line and a patient
507 line, PANx, with idiopathic pancreatitis and a common *CFTR* variant into pancreatic duct like
508 organoids (iPDLO). Upon single cell isolation and characterization using flow-cytomtery, these
509 cells were purely epithelial (i.e. ~99%) based on the presence of the canonical epithelial
510 marker Epithelial cell adhesion molecule (EPCAM). The single cells could be further seeded
511 to generate ring-like epithelial structures i.e. pancreatic ductal like organoids.

512 **e.** Growth characteristics i.e., total area of primary and iPSC-derived pancreatic ductal like
513 organoids (Control and PANx) over extended periods of culture.

514
515
516
517
518
519
520
521
522

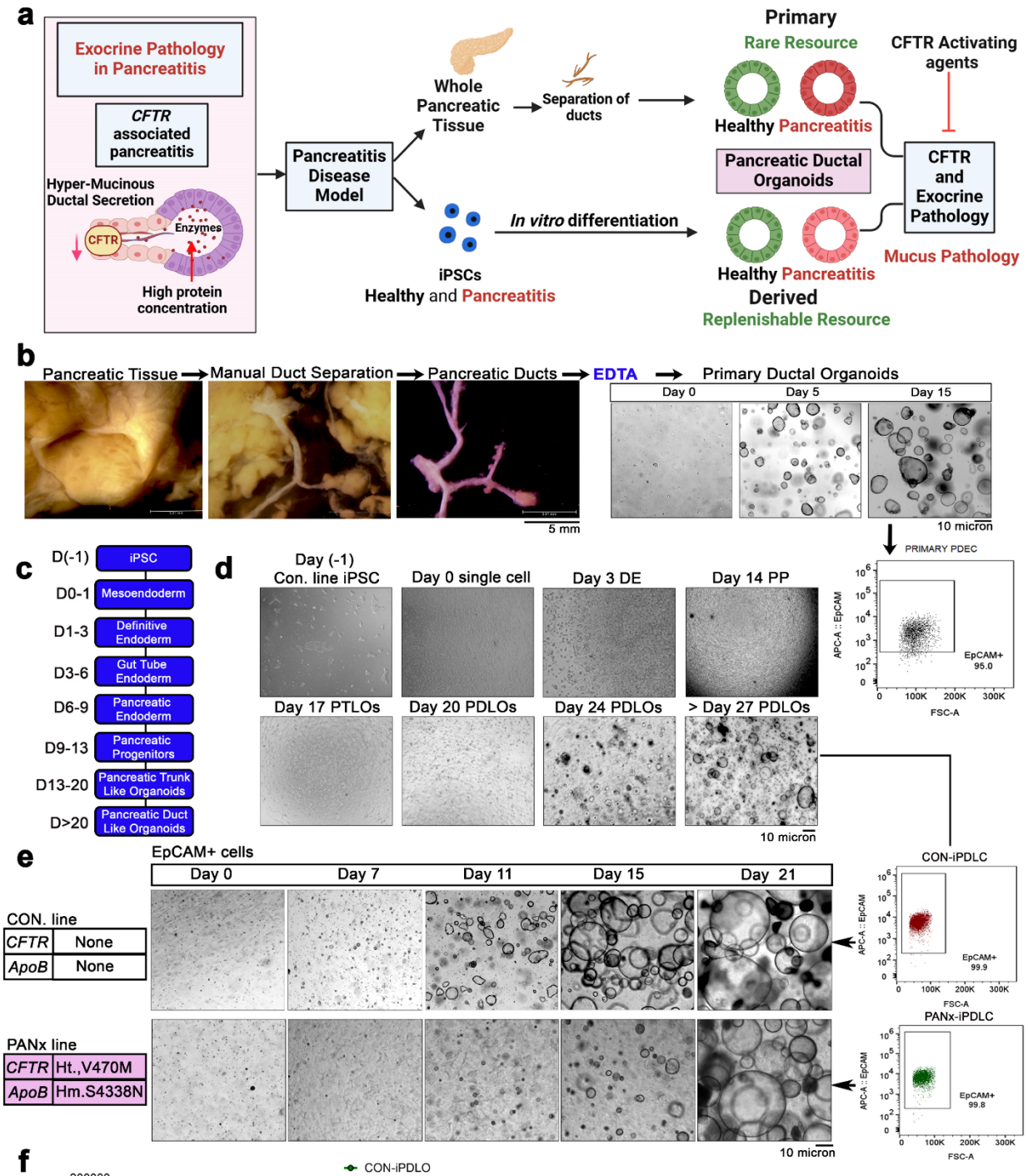
a
Exocrine Pathology in Pancreatitis
CFTR associated pancreatitis
Hyper-Mucinous Ductal Secretion
CFTR
Enzymes
High protein concentration
Pancreatitis Disease Model
Whole Pancreatic Tissue
Separation of ducts
iPSCs
Healthy and Pancreatitis
In vitro differentiation
Primary
Rare Resource
Healthy Pancreatitis
Pancreatic Ductal Organoids
Healthy Pancreatitis
Derived
Replenishable Resource
CFTR Activating agents
CFTR and Exocrine Pathology
Mucus Pathology
b
Pancreatic Tissue
Manual Duct Separation
Pancreatic Ducts
EDTA
Primary Ductal Organoids
Day 0
Day 5
Day 15
5 mm
10 micron
PRIMARY PDEC
EpCAM+ 95.0
c
D(-1) iPSC
D0-1 Mesoendoderm
D1-3 Definitive Endoderm
D3-6 Gut Tube Endoderm
D6-9 Pancreatic Endoderm
D9-13 Pancreatic Progenitors
D13-20 Pancreatic Trunk Like Organoids
D>20 Pancreatic Duct Like Organoids
d
Day (-1) Con. line iPSC
Day 0 single cell
Day 3 DE
Day 14 PP
Day 17 PTLOs
Day 20 PDLOs
Day 24 PDLOs
> Day 27 PDLOs
10 micron
e
EpCAM+ cells
Day 0
Day 7
Day 11
Day 15
Day 21
CON. line
CFTR None
ApoB None
PANx line
CFTR Ht.,V470M
ApoB Hm.S4338N
CON-iPDLC
EpCAM+ 99.9
PANx-iPDLC
EpCAM+ 99.8
10 micron
f
CON-iPDLO
PANx-iPDLO
Primary PDO
PDO organoid area (µm²)
Day

Figure 1

523

524 **Figure 2. Molecular characterization of iPSC-derived pancreatic ductal tissues**

525 **a.** global transcriptomic data were mined to investigate and present normalized expression
526 counts for pancreatic duct specific markers in iPSC-derived ductal cells from control and PANx
527 line and compared to the primary ductal epithelial cells (PDEC) derived from human ductal
528 organoids. None of the markers corresponding to the acinar cells (*AMY*, amylases) or islets,
529 β-cells (*INS*, insulin) were detected in the primary as well as iPSC-derived ductal tissue and
530 the differentiated structures demonstrated pure molecular characteristics of the ductal tissue
531 marked by *CDH1* (E-Cadherin)*, KRT19* (cytokeratin 19) and *ZO1* (zonula occludens 1). Each
532 dot represents a single well containing the ductal organoids for the specified samples. Error
533 bars represent S.E.M.

534 **b.** Graphical scheme on the left shows the regulation of bicarbonate and fluid secretion through
535 the acitvitites of various transporters and channels in pancreatic duct epithelial cells. The bar-
536 graph on the right depicts mRNA expressions for various transporters including CFTR in iPSC-
537 derived ductal tissues i.e., iPDLC from control and PANx lines and compared with PDEC.
538 Each dot represents a single well containing the ductal organoids from which single cells were
539 prepared for mRNA analysis in the specified samples. Error bars represent S.E.M. *P-value*
540 using one-way ANOVA.

541 **c.** scRNA-seq identifies three major populations of cell clusters: ductal mix (four subclusters),
542 proliferating and secretory/mucinous (two subclusters). scRNA-seq data was analyzed using
543 the Seurat v5 package following the standard pre-processing workflow. Doublets were
544 identified and removed prior to downstream analysis. Quality control (QC) was performed to
545 retain only high-quality cells, excluding those with more than 10% mitochondrial gene
546 expression. The data were then normalized, and highly variable features were identified.
547 Principal component analysis (PCA) was conducted, followed by non-linear dimensional
548 reduction using UMAP to visualize cell clustering and transcriptional heterogeneity.

549 The UMAP projection in scRNA-seq of control and PANx cells vividly illustrates that nearly all
550 cells exhibit positive expression for both KRT19 and EPCAM. This ubiquitous co-expression
551 strongly indicates a predominant pancreatic ductal signature, reflecting a fundamental ductalc
552 identity among the sampled cells. The result underscores the robust ductal lineage
553 characteristics within the analyzed cell population and provides critical insights into pancreatic
554 ductal cell's composition.

555 **d.** Immunostaining of the ductal epithelium markers cytokeratin 19 and ZO1 and CFTR in control
556 and PANx iPDLC. DAPI was used as a counterstain.

557

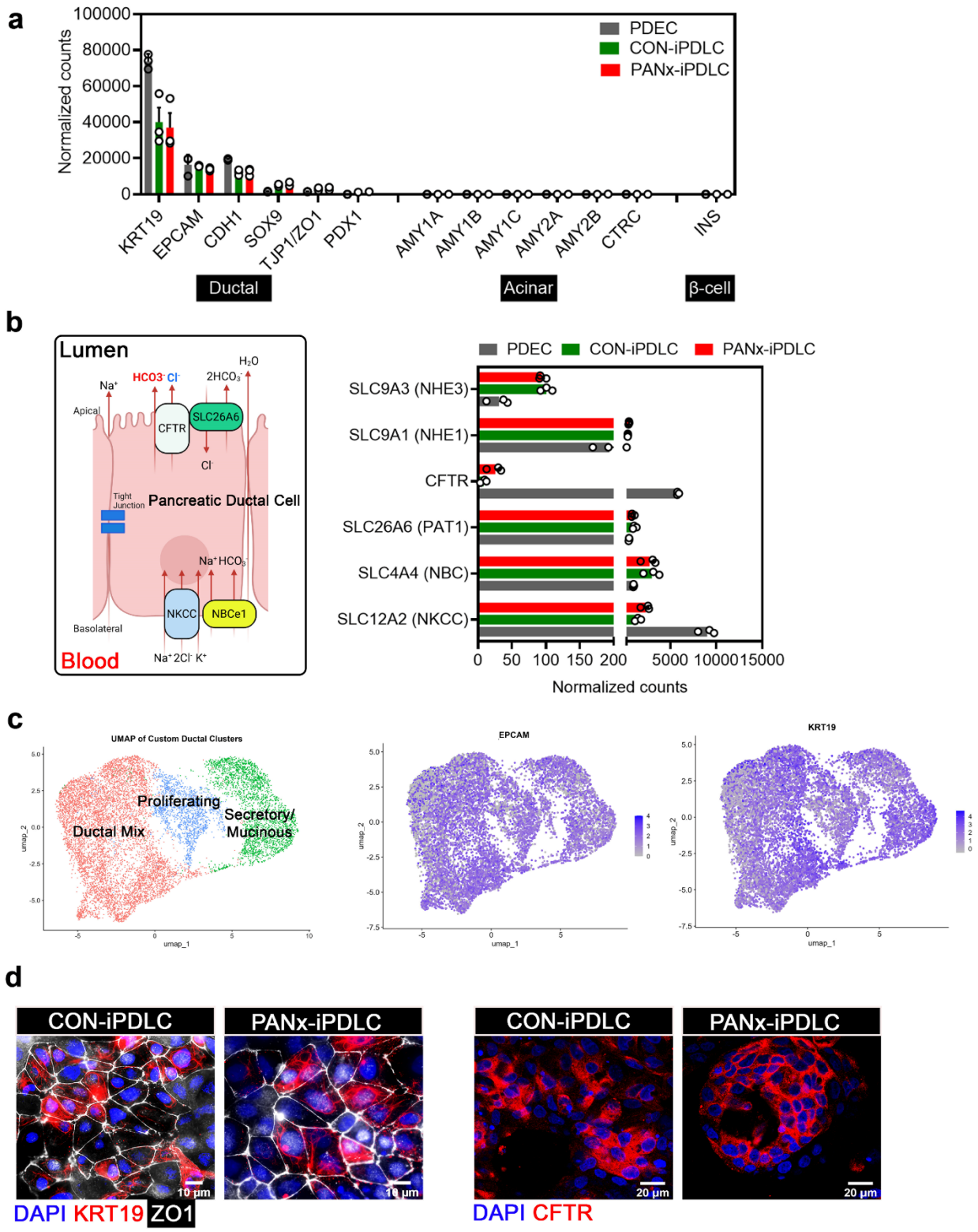
a
Normalized counts
PDEC
CON-iPDLC
PANx-iPDLC
KRT19
EPCAM
CDH1
SOX9
TJP1/ZO1
PDX1
AMY1A
AMY1B
AMY1C
AMY2A
AMY2B
CTRC
INS
Ductal
Acinar
β-cell
b
Lumen
Apical
CFTR
SLC26A6
Pancreatic Ductal Cell
Tight Junction
NKCC
NBCe1
Basolateral
Blood
SLC9A3 (NHE3)
SLC9A1 (NHE1)
CFTR
SLC26A6 (PAT1)
SLC4A4 (NBC)
SLC12A2 (NKCC)
Normalized counts
c
UMAP of Custom Ductal Clusters
Proliferating
Ductal Mix
Secretory/ Mucinous
EPCAM
KRT19
d
CON-iPDLC
PANx-iPDLC
10 µm
20 µm
DAPI KRT19 ZO1
DAPI CFTR

Figure 2

559 **Figure 3. Pancreatitis associated *CFTR* variant caused reduced CFTR activity that could**
560 **be restored using CFTR-activating agents**

561 **a.** Whole-cell recordings from primary PDEC and control iPDLC demonstrating CFTR-inhibitor
562 sensitive currents elicited using FSK (2 μM).
563 **b.** Bar-graph representing iPDLC CFTR current density recorded at -60mV in single cells isolated
564 from primary PDEC and control iPDLC obtained from whole-cell clamp recording as
565 represented in panel E. The measured whole-cell currents were normalized to cell
566 capacitance. Error bars represent S.E.M. Statistical significance was calculated using
567 student's t-test. Each dot represents single cell measurement repeated across three to five
568 independent experiments. Error bars represent S.E.M. *P-value* using student's t-test. ns
569 stands for non-signficant.
570 **c.** Whole-cell recording from PANx iPDLC demonstrating absence of CFTR-inhibitor sensitive
571 currents in response to FSK which were stimulated in the presence of VX-770 (5 μM).
572 **d.** The I-V relationships for CFTR currents in control and PANx iPDLC evoked by 2 μM FSK
573 with or without VX-770 for PANx iPDLC.
574 **e.** Summary of current densities recorded at -60mV for CFTR in control and PANx iPDLCs
575 treated with and without VX-770 in the patch-pipette. The measured whole-cell currents
576 were normalized to cell capacitance. Each dot represents single cell measurement repeated
577 across three to five independent experiments. Error bars represent S.E.M. Statistical
578 significance was calculated using student's t-test.
579 **f.** Short-circuit current (*Isc*) measurements to measure CFTR function in control and and PANx
580 iPDLCs that were differentiated on transwell cultures and stimulated using FSK (2 μM) or
581 VX-770 in the presence or absence of VX-770
582 **g.** Bar-graph shows quantitation of the maximal Δ*Isc* n control and and PANx iPDLCs transwell
583 cultures under different treatment conditions. Each dot represents a single experiment. Error
584 bars represent S.E.M. Statistical significance was calculated using one-way ANOVA.
585 **h.** Bright-field images showing fluid secretion in response to cAMP agonists FSK/IBMX called
586 FSK-induced swelling (FIS) in control and PANx iPDLOs at baseline and 72 h post-stimulation.
587 **i.** The bar-graph represents quantitation of fluid secretion based on total organoid area (μm^2) in
588 the two samples at 0 h and 72 h post-FSK/IBMX treatment. Each dot represents a single
589 organoid, and measurements were repeated across three independent experiments. Error
590 bars represent S.E.M. *P-value* using one-way ANOVA.
591 **j.** Global transcriptomic data were mined to investigate the expression level of various
592 phosphodiesterases (PDEs) in iPSC-derived ductal organoids from control and PANx line.

593 The PDEs can be categorized as cAMP or cGMP-specific or PDEs with dual specificity. PDE
594 inhibitors Rolipram, Zaprinast, and Cilostazol are shown with asterisks to represent their
595 respective specificities towards different PDEs. Each dot represents a single well containing
596 the ductal organoids in the specified samples. Error bars represent S.E.M.

597 **k.** Medium throughput assay with line-graphs representing FIS in control iPDLOs (TOP) and
598 PANx iPDLOs (BOTTOM) in response to simultaneous treatment with PDE inhibitors rolipram
599 (20 μM), zaprinast (50 μM) and cilostazol (20 μM). No FSK treatment with DMSO alone was
600 used as no swelling response control. Error bars represent S.E.M.

601

602

603

604

605

606

607

608

609

610

611

612

613

614

615

616

617

618

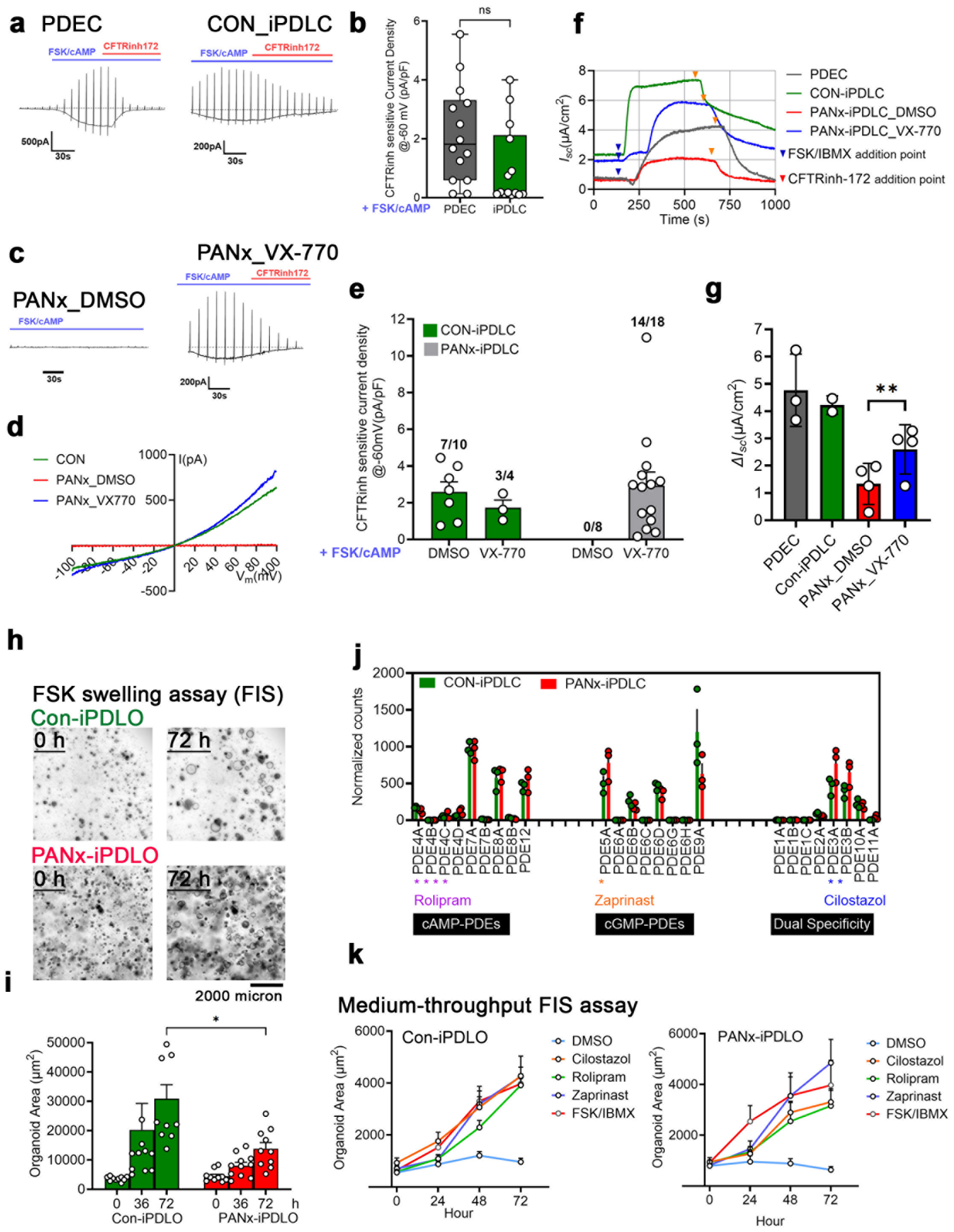
a
PDEC
CON_iPDLC
FSK/cAMP
CFTRinh172
500pA
200pA
30s
b
ns
CFTRinh sensitive Current Density @-60 mV (pA/pF)
+ FSK/cAMP
PDEC
iPDLC
f
PDEC
CON-iPDLC
PANx-iPDLC_DMSO
PANx-iPDLC_VX-770
FSK/IBMX addition point
CFTRinh-172 addition point
Time (s)
c
PANx_VX-770
PANx_DMSO
d
CON
PANx_DMSO
PANx_VX770
I(pA)
e
CON-iPDLC
PANx-iPDLC
CFTRinh sensitive current density @-60mV(pA/pF)
7/10
3/4
0/8
14/18
DMSO
VX-770
g
PDEC
Con-iPDLC
PANx_DMSO
PANx_VX-770
h
FSK swelling assay (FIS)
Con-iPDLO
0 h
72 h
PANx-iPDLO
2000 micron
i
Organoid Area (μm²)
Con-iPDLO
PANx-iPDLO
j
CON-iPDLC
PANx-iPDLC
Normalized counts
Rolipram
Zaprinast
Cilostazol
cAMP-PDEs
cGMP-PDEs
Dual Specificity
k
Medium-throughput FIS assay
Con-iPDLO
PANx-iPDLO
DMSO
Cilostazol
Rolipram
Zaprinast
FSK/IBMX
Hour

Figure 3

619

620 **Figure 4. Ivacaftor reversed mucinous pathological feature in pancreatitis ductal cells**

621 **a.** Normalized expression counts obtained from total transcriptomic data for different major
622 mucins as well as for the regulator of mucins including TFF1, WFDC2 and REG4 in control
623 and PANx iPDLC (± VX-770 (5 μM, 24 h)). Each dot represents a single well containing the
624 ductal organoids in the specified samples. Error bars represent S.E.M. *P-value* was calculated
625 using multiple t-test.

626 **b.** The UMAP visualization for sc-RNAseq data in control and PANx cells revealed that the
627 expression of mucin genes was identified in a unique mucinous-ductal cell population. This
628 spatially confined expression pattern supports the identity and functional specialization of this
629 subset, indicating their distinct role in mucin production and stabilization within the ductal cell
630 population. Violin plots comparing control and PANx conditions for sc-RNAseq data revealed
631 elevated expression of major mucin genes within the mucinous ductal cell population in PANx
632 iPDLC alluding to the presence of a hypermucinous state.

633 **c.** MUC5AC-specific ELISA was used to measure the amount of secreted protein into the media
634 collected from the transwell differentiated cultures of control and PANx iPDLC. Each dot
635 represents a single experiment. Error bars represent the S.E.M. Statistical significance was
636 calculated using one-way ANOVA.

637 **d.** Immunostaining for total mucin using a mucin probe (Biotin-STcE) in the transwell
638 differentiated cultures of control and PANx iPDLC. DAPI was used as nuclear counterstain.
639 3D Mucinous neoplasms were a structural characteristic of differentiated PANx cells, and
640 these structures remarkably disappeared following treatment with VX-770 (5 μM, 24 h).

641 **e.** Confocal images showing positive CDH1 immunostaining for cystic neoplastic structures
642 observed in PANx cells indicating their epithelial origin.

643 **f.** H&E staining shows cystic neoplasms that were only identified in differentiated PANx cells
644 and remarkably disappeared following treatment with VX-770 (5 μM, 24 h). PAS staining
645 shows the presence of distinct mucinous cells and membrane-bound mucins in PANx cells
646 that were not visible following treatment with VX-770 (5 μM, 24 h).

647

648

649

650

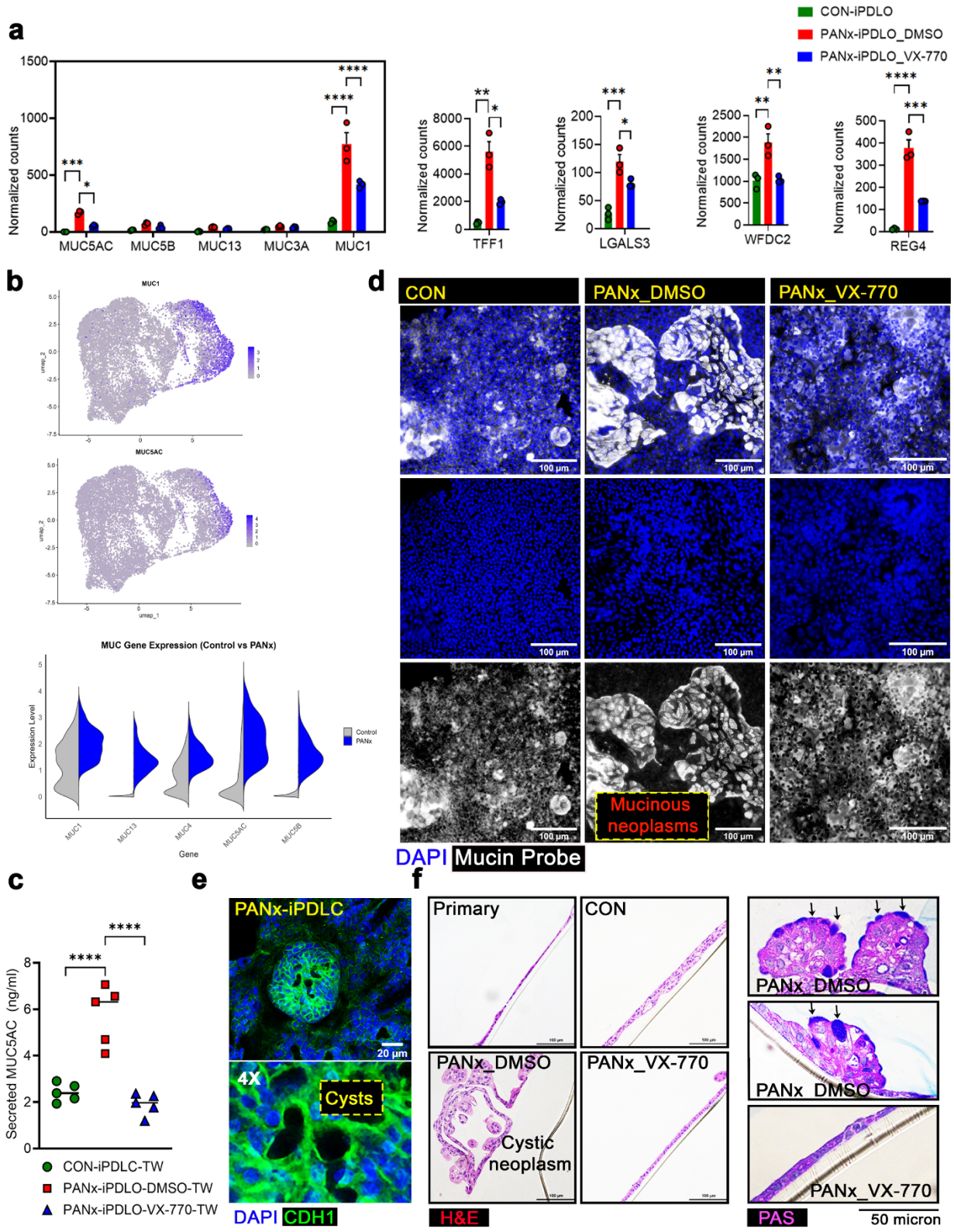
a
CON-iPDLO
PANx-iPDLO_DMSO
PANx-iPDLO_VX-770
Normalized counts
MUC5AC
MUC5B
MUC13
MUC3A
MUC1
TFF1
LGALS3
WFDC2
REG4
b
MUC1
MUC5AC
MUC Gene Expression (Control vs PANx)
Expression Level
Control
PANx
Gene
d
CON
PANx_DMSO
PANx_VX-770
100 µm
Mucinous neoplasms
DAPI Mucin Probe
c
Secreted MUC5AC (ng/ml)
CON-iPDLC-TW
PANx-iPDLO-DMSO-TW
PANx-iPDLO-VX-770-TW
e
PANx-iPDLC
20 µm
4X
Cysts
DAPI CDH1
f
Primary
CON
PANx_DMSO
PANx_VX-770
Cystic neoplasm
H&E
PAS
50 micron

Figure 4

651

652 **Figure 5. Differential gene expression analysis reveals reversal of molecular signature for**
653 **ductal tissue pancreatitis using Ivacaftor**

654 **a.** Differential expression gene (DEG) map for three conditions obtained using total
655 transcriptomic data: Control, PANx-DMSO, and PANx-VX-770 showing clustering of grouped
656 samples and distinct expression landscape with a large overlap between the control and
657 PANX-VX-770 sample groups demonstrating reversal of disease signature for PANx using
658 VX-770. Heatmap was generated using Morpheus application
659 (https://software.broadinstitute.org/morpheus/). Further, these genes were seggregated into
660 CFTR-resonsive and non-responsive based on VX-770 reversible signature in PANx cells
661 relative to the control cells.
662 **b.** Volcano-plot showing top 50 DEGs (UP-Right, DOWN-Left) expressed between control and
663 PANx cells as the comparison group of PANx cells either treated with DMSO alone or VX-770
664 for 24 h. Several top genes showed reversal of expression in the PANx cells upon treatment
665 with VX-770 among which multiple genes belonged to mucins or mucin regulatory genes.
666 Princpal component (PC) analysis plot showing clustering of control and VX-770 treated PANx
667 cells. About 40% of the genes were altered by VX-770 which were differentially expressed in
668 the control cells termed as CFTR responsive with 60% DEGs not affected by VX-770 termed
669 as CFTR non-responsive.
670 **c.** Canonical pathway enrichment revealed top altered pathways (up and down based on z-
671 score) in PANx cells including for O-linked glycosylation which is directly linked to increased
672 synthesis of glycoproteins including mucins and Hif1α signaling directly implicated in
673 pancreatitis assoictaed tissue injury. A highly upregulated pathway signature for neutrophil
674 degranulation suggests ability of PANx cells to promote inflammation.
675 **d.** Top upstream regulators activated or inhibited in PANx cells. Analysis was performed using
676 IPA, Qiagen©.
677 **e.** Activated NFƙb signaling node in PANx cells with a clear reversal of activated signature in
678 VX-770 treated PANx cells. Analysis was performed using IPA, Qiagen©. Identifying legends
679 are included on the bottom right.
680 **f.** DEGs for mucin biosynthesis based on O-linked glycosylation database in lung mucous cell
681 for three conditions obtained using total transcriptomic data: Control, PANx-DMSO, PANx-
682 VX-770 showing enrichment for mucin biosynthesis in PANx that was reversible using VX-
683 770.
684 **g.** Gene expression analysis from whole-transcriptomic sequencing in primary ductal tissues
685 obtained from pediatric patient's remnant TPIAT samples with and without a *CFTR* variant

686 reproduced hypermucinous and secretory profile in pancreatitis samples with the variant
687 similar to the iPSC-derived tissues. The hypermucinous phenotype is additionally supported
688 by highly upregulated expression of TFF1 and REG4 in the cells with *CFTR* variant vs. no
689 variant. Statistical significance was calculated using one-way ANOVA.
690 **h.** Heat-map shows cumulative normalized count score for secreted MUC genes (sum for MUC2,
691 MUC5AC, MUC5B, MUC6, MUC7 and MUC19 and normalized to the control/normal) across
692 iPSC-derived ductal tissues vs. primary tissues under different conditions.

693

694

695

696

697

698

699

700

701

702

703

704

705

706

707

708

709

710

711

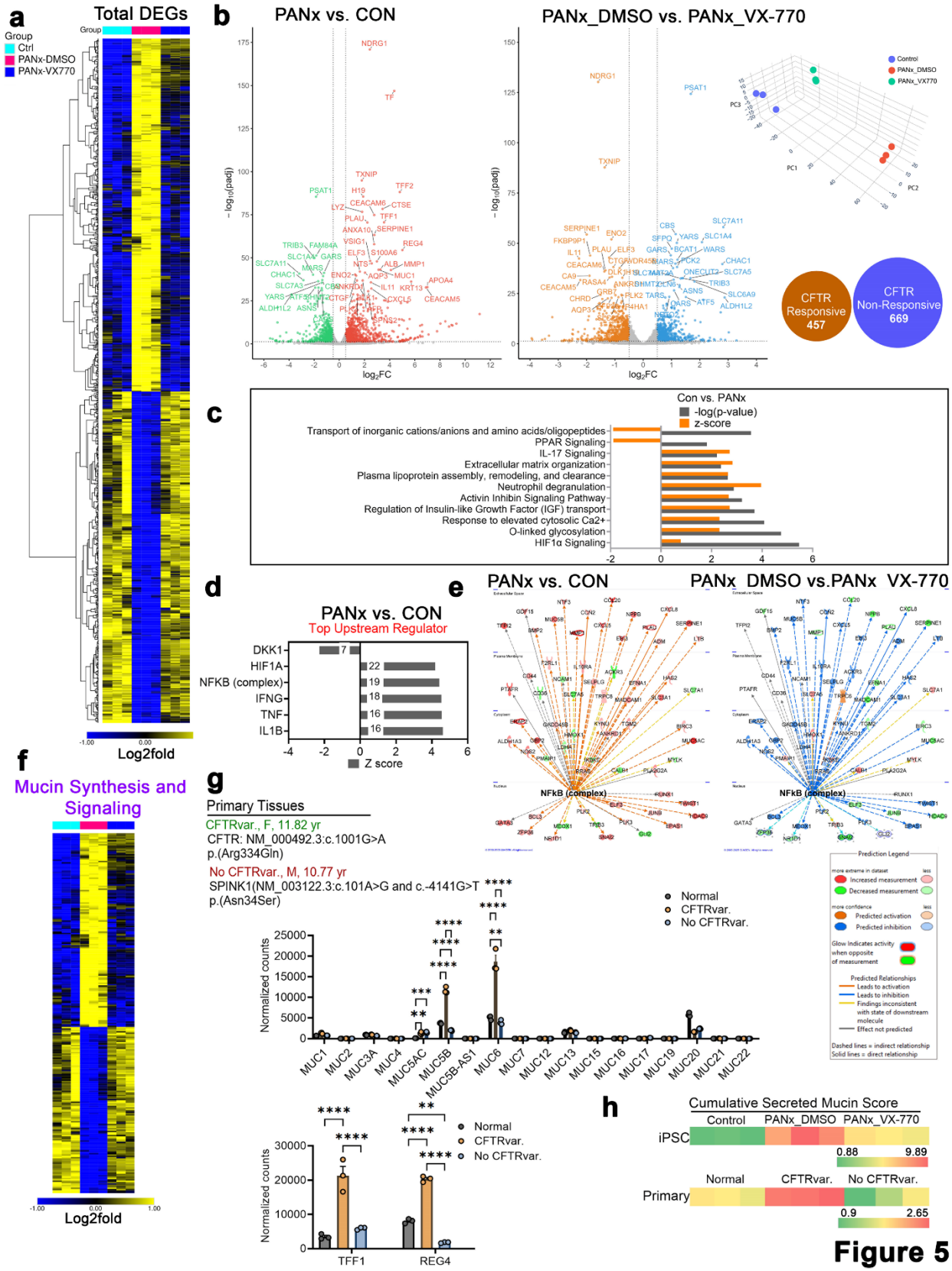
a
Total DEGs
Group
Ctrl
PANx-DMSO
PANx-VX770
Log2fold
b
PANx vs. CON
PANx_DMSO vs. PANx_VX-770
log2FC
CFTR Responsive 457
CFTR Non-Responsive 669
c
Con vs. PANx
-log(p-value)
z-score
Transport of inorganic cations/anions and amino acids/oligopeptides
PPAR Signaling
IL-17 Signaling
Extracellular matrix organization
Plasma lipoprotein assembly, remodeling, and clearance
Neutrophil degranulation
Activin Inhibin Signaling Pathway
Regulation of Insulin-like Growth Factor (IGF) transport
Response to elevated cytosolic Ca2+
O-linked glycosylation
HIF1α Signaling
d
PANx vs. CON
Top Upstream Regulator
DKK1
HIF1A
NFKB (complex)
IFNG
TNF
IL1B
Z score
e
PANx vs. CON
PANx_DMSO vs.PANx_VX-770
NFkB (complex)
Prediction Legend
f
Mucin Synthesis and Signaling
Log2fold
g
Primary Tissues
CFTRvar., F, 11.82 yr
CFTR: NM_000492.3:c.1001G>A
p.(Arg334Gln)
No CFTRvar., M, 10.77 yr
SPINK1(NM_003122.3:c.101A>G and c.-4141G>T
p.(Asn34Ser)
Normal
CFTRvar.
No CFTRvar.
Normalized counts
MUC1
MUC2
MUC3A
MUC4
MUC5AC
MUC5B
MUC5B-AS1
MUC6
MUC7
MUC12
MUC13
MUC15
MUC16
MUC17
MUC19
MUC20
MUC21
MUC22
TFF1
REG4
h
Cumulative Secreted Mucin Score
Control
PANx_DMSO
PANx_VX-770
iPSC
0.88
9.89
Normal
CFTRvar.
No CFTRvar.
Primary
0.9
2.65

Figure 5

713 **Figure 6. Modeling the reaction for hyperamylasemia using a microsystem device**

714 **a.** H&E images of pancreatic tissue showing main duct and interlobular ducts. The pancreatic
715 duct epithelium is highly secretory marked by glycoprotein rich cells which were detected
716 using PAS stain. The intralobular ducts connect to the acini and regulate their function by
717 delivering protein rich ductal secretions.

718 **b.** A microsystem device from Ibidi containing two chambers connected by a narrow channel
719 was used to investigate the effect of the viscous ductal cell fluid (DCF) on acinar cell function.
720 Chamber on the right was used to culture primary acinar channels, and ductal fluid was
721 collected from normal control iPDLC differentiated on transwells. To increase viscosity, the
722 ductal fluid was mixed with glycerol at 10% concentration while keeping the effective ductal
723 fluid composition at 90% same in the samples with and without glycerol.
724 Amylase specific immunistaining on the right shows acinar cells seeded on the microsystem
725 device under the treatment conditions of 100% DCF and 90% DCF,10% glycerol.

726 **c.** The bar-graph represents amylase activity in the fluid collected from the acinar chamber in
727 the samples exposed to complete ductal medium and ductal cell fluid containing 10% glycerol
728 compared to media only. Each dot represents a single sample averaged from a duplicate
729 across independently performed experiments. Error bars represent the S.E.M. Statistical
730 significance was calculated using student's t-test.

731 **d.** The bar-graph represents lactate dehydrogenase (LDH) activity in the fluid collected from the
732 acinar chamber to assess acinar cell condition in the samples exposed to complete ductal
733 medium and ductal fluid containing 10% glycerol compared to media only. Each dot
734 represents a single sample averaged from a duplicate across independently performed
735 experiments. Error bars represent S.E.M. Statistical significance was calculated using
736 student's t-test.

737
738
739
740
741
742
743

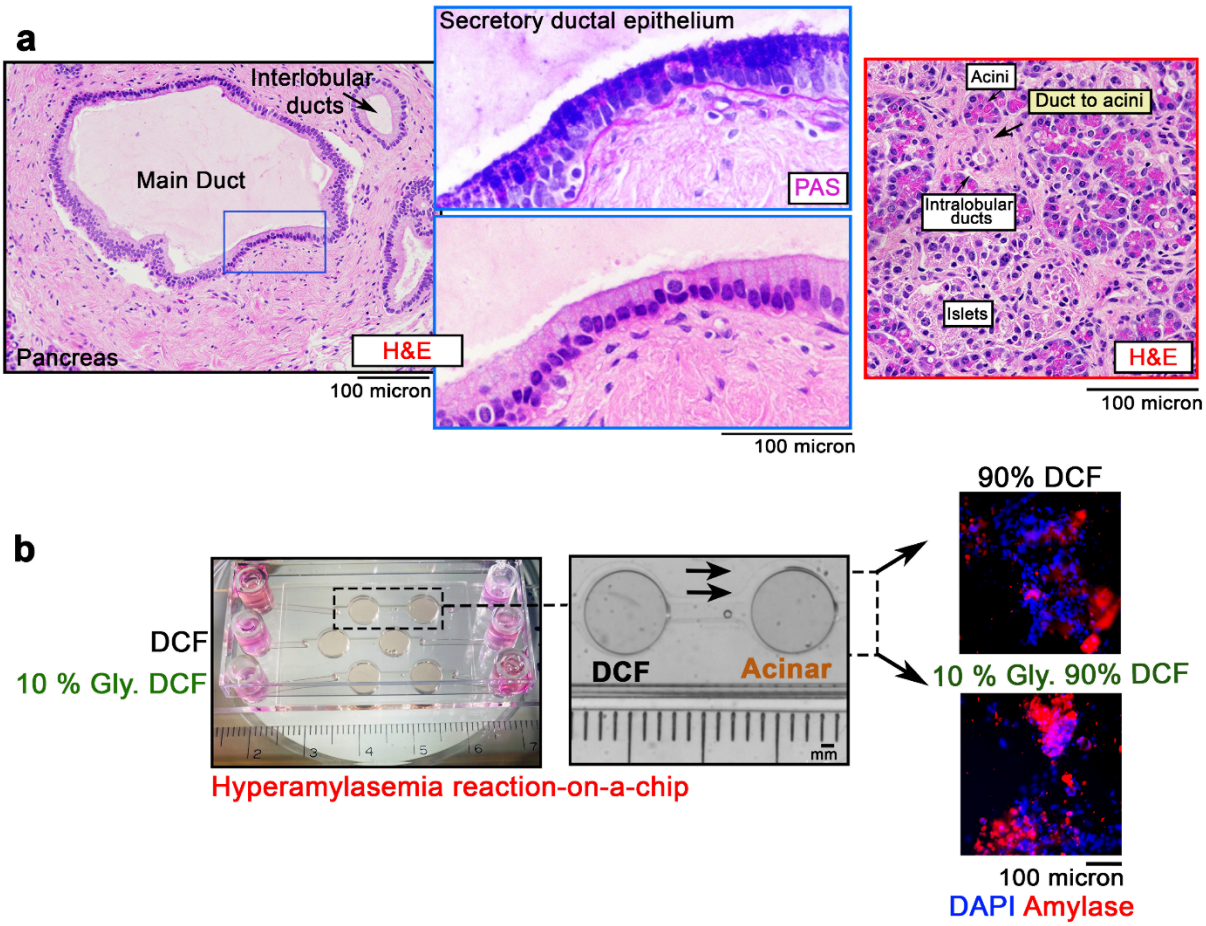
a
Secretory ductal epithelium
Interlobular ducts
Main Duct
PAS
Pancreas
H&E
100 micron
100 micron
Acini
Duct to acini
Intralobular ducts
Islets
H&E
100 micron
b
90% DCF
DCF
10 % Gly. DCF
DCF
Acinar
mm
10 % Gly. 90% DCF
Hyperamylasemia reaction-on-a-chip
100 micron
DAPI Amylase

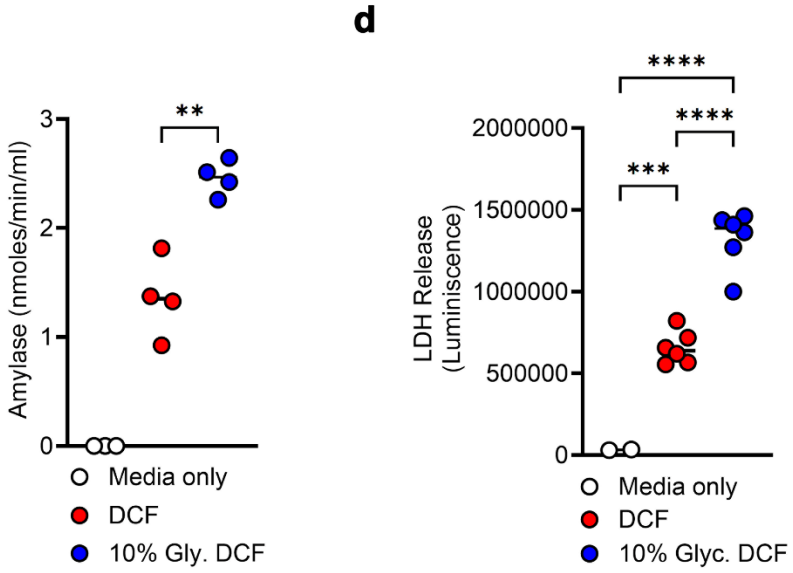
c
Amylase (nmoles/min/ml)
3
2
1
0
**
Media only
DCF
10% Gly. DCF
d
LDH Release (Luminiscence)
2000000
1500000
1000000
500000
0
****
****
***
Media only
DCF
10% Glyc. DCF

Figure 6

Tables

Table 1 and Table 2

References

1 Lee, P. J. & Papachristou, G. I. New insights into acute pancreatitis. *Nat Rev Gastroenterol Hepatol* **16**, 479-496, doi:10.1038/s41575-019-0158-2 (2019).

2 Braganza, J. M., Lee, S. H., McCloy, R. F. & McMahon, M. J. Chronic pancreatitis. *Lancet* **377**, 1184-1197, doi:10.1016/S0140-6736(10)61852-1 (2011).

3 Habtezion, A., Gukovskaya, A. S. & Pandol, S. J. Acute Pancreatitis: A Multifaceted Set of Organelle and Cellular Interactions. *Gastroenterology* **156**, 1941-1950, doi:10.1053/j.gastro.2018.11.082 (2019).

4 Hines, O. J. & Pandol, S. J. Management of chronic pancreatitis. *BMJ* **384**, e070920, doi:10.1136/bmj-2023-070920 (2024).

5 Amann, S. T., Yadav, D., Barmada, M. M., O'Connell, M., Kennard, E. D., Anderson, M., Baillie, J., Sherman, S., Romagnuolo, J., Hawes, R. H., Alkaade, S., Brand, R. E., Lewis, M. D., Gardner, T. B., Gelrud, A., Money, M. E., Banks, P. A., Slivka, A. & Whitcomb, D. C. Physical and mental quality of life in chronic pancreatitis: a case-control study from the North American Pancreatitis Study 2 cohort. *Pancreas* **42**, 293-300, doi:10.1097/MPA.0b013e31826532e7 (2013).

6 Machicado, J. D., Amann, S. T., Anderson, M. A., Abberbock, J., Sherman, S., Conwell, D. L., Cote, G. A., Singh, V. K., Lewis, M. D., Alkaade, S., Sandhu, B. S., Guda, N. M., Muniraj, T., Tang, G., Baillie, J., Brand, R. E., Gardner, T. B., Gelrud, A., Forsmark, C. E., Banks, P. A., Slivka, A., Wilcox, C. M., Whitcomb, D. C. & Yadav, D. Quality of Life in Chronic Pancreatitis is Determined by Constant Pain, Disability/Unemployment, Current Smoking, and Associated Co-Morbidities. *Am J Gastroenterol* **112**, 633-642, doi:10.1038/ajg.2017.42 (2017).

7 Singh, V. K., Yadav, D. & Garg, P. K. Diagnosis and Management of Chronic Pancreatitis: A Review. *JAMA* **322**, 2422-2434, doi:10.1001/jama.2019.19411 (2019).

8 Schneider, A., Lohr, J. M. & Singer, M. V. The M-ANNHEIM classification of chronic pancreatitis: introduction of a unifying classification system based on a review of previous classifications of the disease. *J Gastroenterol* **42**, 101-119, doi:10.1007/s00535-006-1945-4 (2007).

9 Sankaran, S. J., Xiao, A. Y., Wu, L. M., Windsor, J. A., Forsmark, C. E. & Petrov, M. S. Frequency of progression from acute to chronic pancreatitis and risk factors: a meta-analysis. *Gastroenterology* **149**, 1490-1500 e1491, doi:10.1053/j.gastro.2015.07.066 (2015).

10 Hegyi, P. J., Soos, A., Toth, E., Ebert, A., Venglovecz, V., Marta, K., Matrai, P., Miko, A., Bajor, J., Sarlos, P., Vincze, A., Halasz, A., Izbeki, F., Szepes, Z., Czako, L., Kovacs, G., Papp, M., Dubravcsik, Z., Varga, M., Hamvas, J., Nemeth, B. C., Macarie, M., Ince, A. T., Bordin, D. S., Dubtsova, E. A., Kiryukova, M. A., Khatkov, I. E., Bideeva, T., Mickevicius, A., Ramirez-Maldonado, E., Sallinen, V., Eross, B., Pecsi, D., Szentesi, A., Parniczky, A., Tiszlavicz, L. & Hegyi, P. Evidence for diagnosis of early chronic pancreatitis after three episodes of acute pancreatitis: a cross-sectional multicentre international study with experimental animal model. *Sci Rep* **11**, 1367, doi:10.1038/s41598-020-80532-6 (2021).

11 Hegyi, P., Wilschanski, M., Muallem, S., Lukacs, G. L., Sahin-Toth, M., Uc, A., Gray, M. A., Rakonczay, Z., Jr. & Maleth, J. CFTR: A New Horizon in the Pathomechanism and Treatment of Pancreatitis. *Rev Physiol Biochem Pharmacol* **170**, 37-66, doi:10.1007/112_2015_5002 (2016).

12 Cohn, J. A., Friedman, K. J., Noone, P. G., Knowles, M. R., Silverman, L. M. & Jowell, P. S. Relation between mutations of the cystic fibrosis gene and idiopathic pancreatitis. *N Engl J Med* **339**, 653-658, doi:10.1056/NEJM199809033391002 (1998).

13 Miller, A. C., Comellas, A. P., Hornick, D. B., Stoltz, D. A., Cavanaugh, J. E., Gerke, A. K., Welsh, M. J., Zabner, J. & Polgreen, P. M. Cystic fibrosis carriers are at increased risk for a wide range of cystic fibrosis-related conditions. *Proc Natl Acad Sci U S A* **117**, 1621-1627, doi:10.1073/pnas.1914912117 (2020).

14 Hooks, G., Lu, H., Eaton, A., Trikudanathan, G., Downs, E., Freeman, M. L., Schwarzenberg, S. J., Pruett, T. L., Chinnakotla, S., Ramanathan, K., Beilman, G. J. & Bellin, M. D. Addressing long-term mortality risk in patients undergoing total pancreatectomy with islet autotransplant (TPIAT): causes of death and risk factors. *HPB (Oxford)* **26**, 664-673, doi:10.1016/j.hpb.2024.02.002 (2024).

15 Maleth, J., Balazs, A., Pallagi, P., Balla, Z., Kui, B., Katona, M., Judak, L., Nemeth, I., Kemeny, L. V., Rakonczay, Z., Jr., Venglovecz, V., Foldesi, I., Peto, Z., Somoracz, A., Borka, K., Perdomo, D., Lukacs, G. L., Gray, M. A., Monterisi, S., Zaccolo, M., Sendler, M., Mayerle, J., Kuhn, J. P., Lerch, M. M., Sahin-Toth, M. & Hegyi, P. Alcohol disrupts levels and function of the cystic fibrosis transmembrane conductance regulator to promote development of pancreatitis. *Gastroenterology* **148**, 427-439 e416, doi:10.1053/j.gastro.2014.11.002 (2015).

16 Takacs, T., Rosztoczy, A., Maleth, J., Rakonczay, Z., Jr. & Hegyi, P. Intraductal acidosis in acute biliary pancreatitis. *Pancreatology* **13**, 333-335, doi:10.1016/j.pan.2013.05.011 (2013).

17 Wittel, U. A., Singh, A. P., Henley, B. J., Andrianifahanana, M., Akhter, M. P., Cullen, D. M. & Batra, S. K. Cigarette smoke-induced differential expression of the genes involved in exocrine function of the rat pancreas. *Pancreas* **33**, 364-370, doi:10.1097/01.mpa.0000240601.80570.31 (2006).

18 Shik Mun, K., Arora, K., Huang, Y., Yang, F., Yarlagadda, S., Ramananda, Y., Abu-El-Haija, M., Palermo, J. J., Appakalai, B. N., Nathan, J. D. & Naren, A. P. Patient-derived pancreas-on-a-chip to model cystic fibrosis-related disorders. *Nat Commun* **10**, 3124, doi:10.1038/s41467-019-11178-w (2019).

19 O'Malley, Y., Rotti, P. G., Thornell, I. M., Vanegas Calderon, O. G., Febres-Aldana, C., Durham, K., Yao, J., Li, X., Zhu, Z., Norris, A. W., Zabner, J., Engelhardt, J. F. & Uc, A. Development of a polarized pancreatic ductular cell epithelium for physiological studies. *J Appl Physiol (1985)* **125**, 97-106, doi:10.1152/japplphysiol.00043.2018 (2018).

20 Gibson-Corley, K. N., Meyerholz, D. K. & Engelhardt, J. F. Pancreatic pathophysiology in cystic fibrosis. *J Pathol* **238**, 311-320, doi:10.1002/path.4634 (2016).

21 Abu-El-Haija, M., Sinkora, M., Meyerholz, D. K., Welsh, M. J., McCray, P. B., Jr., Butler, J. & Uc, A. An activated immune and inflammatory response targets the pancreas of newborn pigs with cystic fibrosis. *Pancreatology* **11**, 506-515, doi:10.1159/000332582 (2011).

22 Singh, V. K. & Schwarzenberg, S. J. Pancreatic insufficiency in Cystic Fibrosis. *J Cyst Fibros* **16 Suppl 2**, S70-S78, doi:10.1016/j.jcf.2017.06.011 (2017).

23 Yamaguchi, Y., Matsuno, K., Goto, M. & Ogawa, M. In situ kinetics of acinar, duct, and inflammatory cells in duct ligation-induced pancreatitis in rats. *Gastroenterology* **104**, 1498-1506, doi:10.1016/0016-5085(93)90362-g (1993).

24 Rankin, M. M., Wilbur, C. J., Rak, K., Shields, E. J., Granger, A. & Kushner, J. A. beta-Cells are not generated in pancreatic duct ligation-induced injury in adult mice. *Diabetes* **62**, 1634-1645, doi:10.2337/db12-0848 (2013).

25 Middleton, P. G., Mall, M. A., Drevinek, P., Lands, L. C., McKone, E. F., Polineni, D., Ramsey, B. W., Taylor-Cousar, J. L., Tullis, E., Vermeulen, F., Marigowda, G., McKee, C. M., Moskowitz, S. M., Nair, N., Savage, J., Simard, C., Tian, S., Waltz, D., Xuan, F., Rowe, S. M., Jain, R. & Group, V. X. S. Elexacaftor-Tezacaftor-Ivacaftor for Cystic Fibrosis with a Single Phe508del Allele. *N Engl J Med* **381**, 1809-1819, doi:10.1056/NEJMoa1908639 (2019).

26 Ramsey, B. W., Davies, J., McElvaney, N. G., Tullis, E., Bell, S. C., Drevinek, P., Griese, M., McKone, E. F., Wainwright, C. E., Konstan, M. W., Moss, R., Ratjen, F., Sermet-Gaudelus, I., Rowe, S. M., Dong, Q., Rodriguez, S., Yen, K., Ordonez, C., Elborn, J. S. & Group, V. X. S. A CFTR potentiator in patients with cystic fibrosis and the G551D mutation. *N Engl J Med* **365**, 1663-1672, doi:10.1056/NEJMoa1105185 (2011).

27 Tang, T. Y., Cruz, V. B. & Konczal, L. L. Idiopathic chronic pancreatitis treated with ivacaftor in a CFTR carrier with methylmalonic acidemia. *J Cyst Fibros* **21**, 603-605, doi:10.1016/j.jcf.2021.12.013 (2022).
28 Akshintala, V. S., Kamal, A., Faghih, M., Cutting, G. R., Cebotaru, L., West, N. E., Jennings, M. T., Dezube, R., Whitcomb, D. C., Lechtzin, N., Merlo, C. A. & Singh, V. K. Cystic fibrosis transmembrane conductance regulator modulators reduce the risk of recurrent acute pancreatitis among adult patients with pancreas sufficient cystic fibrosis. *Pancreatology* **19**, 1023-1026, doi:10.1016/j.pan.2019.09.014 (2019).
29 Angyal, D., Kleinfelder, K., Ciciriello, F., Groeneweg, T. A., De Marchi, G., de Pretis, N., Bernardoni, L., Rodella, L., Tomba, F., De Angelis, P., Surace, C., Pintani, E., Alghisi, F., de Jonge, H. R., Melotti, P., Sorio, C., Lucidi, V., Bijvelds, M. J. C. & Frulloni, L. CFTR function is impaired in a subset of patients with pancreatitis carrying rare CFTR variants. *Pancreatology* **24**, 394-403, doi:10.1016/j.pan.2024.03.005 (2024).
30 Seymour, P. A., Freude, K. K., Tran, M. N., Mayes, E. E., Jensen, J., Kist, R., Scherer, G. & Sander, M. SOX9 is required for maintenance of the pancreatic progenitor cell pool. *Proc Natl Acad Sci U S A* **104**, 1865-1870, doi:10.1073/pnas.0609217104 (2007).
31 Cogger, K. F., Sinha, A., Sarangi, F., McGaugh, E. C., Saunders, D., Dorrell, C., Mejia-Guerrero, S., Aghazadeh, Y., Rourke, J. L., Screaton, R. A., Grompe, M., Streeter, P. R., Powers, A. C., Brissova, M., Kislinger, T. & Nostro, M. C. Glycoprotein 2 is a specific cell surface marker of human pancreatic progenitors. *Nat Commun* **8**, 331, doi:10.1038/s41467-017-00561-0 (2017).
32 Breunig, M., Merkle, J., Wagner, M., Melzer, M. K., Barth, T. F. E., Engleitner, T., Krumm, J., Wiedenmann, S., Cohrs, C. M., Perkhofer, L., Jain, G., Kruger, J., Hermann, P. C., Schmid, M., Madacsy, T., Varga, A., Griger, J., Azoitei, N., Muller, M., Wessely, O., Robey, P. G., Heller, S., Dantes, Z., Reichert, M., Gunes, C., Bolenz, C., Kuhn, F., Maleth, J., Speier, S., Liebau, S., Sipos, B., Kuster, B., Seufferlein, T., Rad, R., Meier, M., Hohwieler, M. & Kleger, A. Modeling plasticity and dysplasia of pancreatic ductal organoids derived from human pluripotent stem cells. *Cell Stem Cell* **28**, 1105-1124 e1119, doi:10.1016/j.stem.2021.03.005 (2021).
33 Breunig, M., Merkle, J., Melzer, M. K., Heller, S., Seufferlein, T., Meier, M., Hohwieler, M. & Kleger, A. Differentiation of human pluripotent stem cells into pancreatic duct-like organoids. *STAR Protoc* **2**, 100913, doi:10.1016/j.xpro.2021.100913 (2021).
34 Rotti, P. G., Yi, Y., Gasser, G., Yuan, F., Sun, X., Apak-Evans, I., Wu, P., Liu, G., Choi, S., Reeves, R., Scioneaux, A. E., Zhang, Y., Winter, M., Liang, B., Cunicelli, N., Uc, A., Norris, A. W., Sussel, L., Wells, K. L. & Engelhardt, J. F. CFTR represses a PDX1 axis to govern pancreatic ductal cell fate. *iScience* **27**, 111393, doi:10.1016/j.isci.2024.111393 (2024).
35 Boucher, R. C. Muco-Obstructive Lung Diseases. *N Engl J Med* **380**, 1941-1953, doi:10.1056/NEJMra1813799 (2019).
36 Zhou, D., Bai, R. & Wang, L. The Cystic Fibrosis Transmembrane Conductance Regulator 470 Met Allele Is Associated with an Increased Risk of Chronic Pancreatitis in Both Asian and Caucasian Populations: A Meta-Analysis. *Genet Test Mol Biomarkers* **24**, 24-32, doi:10.1089/gtmb.2019.0199 (2020).
37 Ideozu, J. E., Liu, M., Riley-Gillis, B. M., Paladugu, S. R., Rahimov, F., Krishnan, P., Tripathi, R., Dorr, P., Levy, H., Singh, A., Waring, J. F. & Vasanthakumar, A. Diversity of CFTR variants across ancestries characterized using 454,727 UK biobank whole exome sequences. *Genome Med* **16**, 43, doi:10.1186/s13073-024-01316-5 (2024).
38 Boj, S. F., Hwang, C. I., Baker, L. A., Chio, II, Engle, D. D., Corbo, V., Jager, M., Ponz-Sarvise, M., Tiriac, H., Spector, M. S., Gracanin, A., Oni, T., Yu, K. H., van Boxtel, R., Huch, M., Rivera, K. D., Wilson, J. P., Feigin, M. E., Ohlund, D., Handly-Santana, A., Ardito-Abraham, C. M., Ludwig, M., Elyada, E., Alagesan, B., Biffi, G., Yordanov, G. N., Delcuze, B., Creighton, B., Wright, K., Park, Y.,

Morsink, F. H., Molenaar, I. Q., Borel Rinkes, I. H., Cuppen, E., Hao, Y., Jin, Y., Nijman, I. J., Iacobuzio-Donahue, C., Leach, S. D., Pappin, D. J., Hammell, M., Klimstra, D. S., Basturk, O., Hruban, R. H., Offerhaus, G. J., Vries, R. G., Clevers, H. & Tuveson, D. A. Organoid models of human and mouse ductal pancreatic cancer. *Cell* **160**, 324-338, doi:10.1016/j.cell.2014.12.021 (2015).

39 Yu, H., Burton, B., Huang, C. J., Worley, J., Cao, D., Johnson, J. P., Jr., Urrutia, A., Joubran, J., Seepersaud, S., Sussky, K., Hoffman, B. J. & Van Goor, F. Ivacaftor potentiation of multiple CFTR channels with gating mutations. *J Cyst Fibros* **11**, 237-245, doi:10.1016/j.jcf.2011.12.005 (2012).

40 Van Goor, F., Hadida, S., Grootenhuis, P. D., Burton, B., Cao, D., Neuberger, T., Turnbull, A., Singh, A., Joubran, J., Hazlewood, A., Zhou, J., McCartney, J., Arumugam, V., Decker, C., Yang, J., Young, C., Olson, E. R., Wine, J. J., Frizzell, R. A., Ashlock, M. & Negulescu, P. Rescue of CF airway epithelial cell function in vitro by a CFTR potentiator, VX-770. *Proc Natl Acad Sci U S A* **106**, 18825-18830, doi:10.1073/pnas.0904709106 (2009).

41 Liu, F., Zhang, Z., Levit, A., Levring, J., Touhara, K. K., Shoichet, B. K. & Chen, J. Structural identification of a hotspot on CFTR for potentiation. *Science* **364**, 1184-1188, doi:10.1126/science.aaw7611 (2019).

42 Dekkers, J. F., Berkers, G., Kruisselbrink, E., Vonk, A., de Jonge, H. R., Janssens, H. M., Bronsveld, I., van de Graaf, E. A., Nieuwenhuis, E. E., Houwen, R. H., Vleggaar, F. P., Escher, J. C., de Rijke, Y. B., Majoor, C. J., Heijerman, H. G., de Winter-de Groot, K. M., Clevers, H., van der Ent, C. K. & Beekman, J. M. Characterizing responses to CFTR-modulating drugs using rectal organoids derived from subjects with cystic fibrosis. *Sci Transl Med* **8**, 344ra384, doi:10.1126/scitranslmed.aad8278 (2016).

43 Dekkers, J. F., Wiegerinck, C. L., de Jonge, H. R., Bronsveld, I., Janssens, H. M., de Winter-de Groot, K. M., Brandsma, A. M., de Jong, N. W., Bijvelds, M. J., Scholte, B. J., Nieuwenhuis, E. E., van den Brink, S., Clevers, H., van der Ent, C. K., Middendorp, S. & Beekman, J. M. A functional CFTR assay using primary cystic fibrosis intestinal organoids. *Nat Med* **19**, 939-945, doi:10.1038/nm.3201 (2013).

44 Kanehiro, A., Ikemura, T., Makela, M. J., Lahn, M., Joetham, A., Dakhama, A. & Gelfand, E. W. Inhibition of phosphodiesterase 4 attenuates airway hyperresponsiveness and airway inflammation in a model of secondary allergen challenge. *Am J Respir Crit Care Med* **163**, 173-184, doi:10.1164/ajrccm.163.1.2001118 (2001).

45 Goldstein, I., Lue, T. F., Padma-Nathan, H., Rosen, R. C., Steers, W. D. & Wicker, P. A. Oral sildenafil in the treatment of erectile dysfunction. Sildenafil Study Group. *N Engl J Med* **338**, 1397-1404, doi:10.1056/NEJM199805143382001 (1998).

46 Guazzi, M. Clinical use of phosphodiesterase-5 inhibitors in chronic heart failure. *Circ Heart Fail* **1**, 272-280, doi:10.1161/CIRCHEARTFAILURE.108.802116 (2008).

47 Toward, T. J., Smith, N. & Broadley, K. J. Effect of phosphodiesterase-5 inhibitor, sildenafil (Viagra), in animal models of airways disease. *Am J Respir Crit Care Med* **169**, 227-234, doi:10.1164/rccm.200211-1372OC (2004).

48 Birk, S., Kruuse, C., Petersen, K. A., Jonassen, O., Tfelt-Hansen, P. & Olesen, J. The phosphodiesterase 3 inhibitor cilostazol dilates large cerebral arteries in humans without affecting regional cerebral blood flow. *J Cereb Blood Flow Metab* **24**, 1352-1358, doi:10.1097/01.WCB.0000143536.22131.D7 (2004).

49 Morrison, C. B., Markovetz, M. R. & Ehre, C. Mucus, mucins, and cystic fibrosis. *Pediatr Pulmonol* **54 Suppl 3**, S84-S96, doi:10.1002/ppul.24530 (2019).

50 Hu, J., Shi, Y., Wang, C., Wan, H., Wu, D., Wang, H. & Peng, X. Role of intestinal trefoil factor in protecting intestinal epithelial cells from burn-induced injury. *Sci Rep* **8**, 3201, doi:10.1038/s41598-018-21282-4 (2018).

51 Soutto, M., Chen, Z., Bhat, A. A., Wang, L., Zhu, S., Gomaa, A., Bates, A., Bhat, N. S., Peng, D., Belkhiri, A., Piazuelo, M. B., Washington, M. K., Steven, X. C., Peek, R., Jr. & El-Rifai, W. Activation of STAT3 signaling is mediated by TFF1 silencing in gastric neoplasia. *Nat Commun* **10**, 3039, doi:10.1038/s41467-019-11011-4 (2019).
52 Argueso, P., Guzman-Aranguez, A., Mantelli, F., Cao, Z., Ricciuto, J. & Panjwani, N. Association of cell surface mucins with galectin-3 contributes to the ocular surface epithelial barrier. *J Biol Chem* **284**, 23037-23045, doi:10.1074/jbc.M109.033332 (2009).
53 Parikh, K., Antanaviciute, A., Fawkner-Corbett, D., Jagielowicz, M., Aulicino, A., Lagerholm, C., Davis, S., Kinchen, J., Chen, H. H., Alham, N. K., Ashley, N., Johnson, E., Hublitz, P., Bao, L., Lukomska, J., Andev, R. S., Bjorklund, E., Kessler, B. M., Fischer, R., Goldin, R., Koohy, H. & Simmons, A. Colonic epithelial cell diversity in health and inflammatory bowel disease. *Nature* **567**, 49-55, doi:10.1038/s41586-019-0992-y (2019).
54 Sasaki, N., Sachs, N., Wiebrands, K., Ellenbroek, S. I., Fumagalli, A., Lyubimova, A., Begthel, H., van den Born, M., van Es, J. H., Karthaus, W. R., Li, V. S., Lopez-Iglesias, C., Peters, P. J., van Rheenen, J., van Oudenaarden, A. & Clevers, H. Reg4+ deep crypt secretory cells function as epithelial niche for Lgr5+ stem cells in colon. *Proc Natl Acad Sci U S A* **113**, E5399-5407, doi:10.1073/pnas.1607327113 (2016).
55 Fritz, S., Warshaw, A. L. & Thayer, S. P. Management of mucin-producing cystic neoplasms of the pancreas. *Oncologist* **14**, 125-136, doi:10.1634/theoncologist.2008-0200 (2009).
56 Conlon, K. C. Intraductal papillary mucinous tumors of the pancreas. *J Clin Oncol* **23**, 4518-4523, doi:10.1200/JCO.2005.22.517 (2005).
57 Ryan, K. M., Phillips, A. C. & Vousden, K. H. Regulation and function of the p53 tumor suppressor protein. *Curr Opin Cell Biol* **13**, 332-337, doi:10.1016/s0955-0674(00)00216-7 (2001).
58 Sausen, M., Phallen, J., Adleff, V., Jones, S., Leary, R. J., Barrett, M. T., Anagnostou, V., Parpart-Li, S., Murphy, D., Kay Li, Q., Hruban, C. A., Scharpf, R., White, J. R., O'Dwyer, P. J., Allen, P. J., Eshleman, J. R., Thompson, C. B., Klimstra, D. S., Linehan, D. C., Maitra, A., Hruban, R. H., Diaz, L. A., Jr., Von Hoff, D. D., Johansen, J. S., Drebin, J. A. & Velculescu, V. E. Clinical implications of genomic alterations in the tumour and circulation of pancreatic cancer patients. *Nat Commun* **6**, 7686, doi:10.1038/ncomms8686 (2015).
59 Ren, B., Liu, X. & Suriawinata, A. A. Pancreatic Ductal Adenocarcinoma and Its Precursor Lesions: Histopathology, Cytopathology, and Molecular Pathology. *Am J Pathol* **189**, 9-21, doi:10.1016/j.ajpath.2018.10.004 (2019).
60 Talar-Wojnarowska, R., Pazurek, M., Durko, L., Degowska, M., Rydzewska, G., Smigielski, J., Janiak, A., Olakowski, M., Lampe, P., Grzelak, P., Stefanczyk, L. & Malecka-Panas, E. Pancreatic cyst fluid analysis for differential diagnosis between benign and malignant lesions. *Oncol Lett* **5**, 613-616, doi:10.3892/ol.2012.1071 (2013).
61 Koch, S., Capaldo, C. T., Samarin, S., Nava, P., Neumaier, I., Skerra, A., Sacks, D. B., Parkos, C. A. & Nusrat, A. Dkk-1 inhibits intestinal epithelial cell migration by attenuating directional polarization of leading edge cells. *Mol Biol Cell* **20**, 4816-4825, doi:10.1091/mbc.e09-05-0415 (2009).
62 Saluja, A., Dudeja, V., Dawra, R. & Sah, R. P. Early Intra-Acinar Events in Pathogenesis of Pancreatitis. *Gastroenterology* **156**, 1979-1993, doi:10.1053/j.gastro.2019.01.268 (2019).
63 Gorelick, F. S. & Thrower, E. The acinar cell and early pancreatitis responses. *Clin Gastroenterol Hepatol* **7**, S10-14, doi:10.1016/j.cgh.2009.07.036 (2009).
64 Gukovskaya, A. S., Gukovsky, I., Zaninovic, V., Song, M., Sandoval, D., Gukovsky, S. & Pandol, S. J. Pancreatic acinar cells produce, release, and respond to tumor necrosis factor-alpha. Role in regulating cell death and pancreatitis. *J Clin Invest* **100**, 1853-1862, doi:10.1172/JCI119714 (1997).

65 Bhatia, M., Brady, M., Shokuhi, S., Christmas, S., Neoptolemos, J. P. & Slavin, J. Inflammatory mediators in acute pancreatitis. *J Pathol* **190**, 117-125, doi:10.1002/(SICI)1096-9896(200002)190:2<117::AID-PATH494>3.0.CO;2-K (2000).
66 Huang, H., Liu, Y., Daniluk, J., Gaiser, S., Chu, J., Wang, H., Li, Z. S., Logsdon, C. D. & Ji, B. Activation of nuclear factor-kappaB in acinar cells increases the severity of pancreatitis in mice. *Gastroenterology* **144**, 202-210, doi:10.1053/j.gastro.2012.09.059 (2013).
67 Li, N., Wu, X., Holzer, R. G., Lee, J. H., Todoric, J., Park, E. J., Ogata, H., Gukovskaya, A. S., Gukovsky, I., Pizzo, D. P., VandenBerg, S., Tarin, D., Atay, C., Arkan, M. C., Deerinck, T. J., Moscat, J., Diaz-Meco, M., Dawson, D., Erkan, M., Kleeff, J. & Karin, M. Loss of acinar cell IKKalpha triggers spontaneous pancreatitis in mice. *J Clin Invest* **123**, 2231-2243, doi:10.1172/JCI64498 (2013).
68 Gukovskaya, A. S. & Gukovsky, I. Which way to die: the regulation of acinar cell death in pancreatitis by mitochondria, calcium, and reactive oxygen species. *Gastroenterology* **140**, 1876-1880, doi:10.1053/j.gastro.2011.04.025 (2011).
69 Lam, R. & Muniraj, T. in *StatPearls* (2025).
70 Grady, T., Mah'Moud, M., Otani, T., Rhee, S., Lerch, M. M. & Gorelick, F. S. Zymogen proteolysis within the pancreatic acinar cell is associated with cellular injury. *Am J Physiol* **275**, G1010-1017, doi:10.1152/ajpgi.1998.275.5.G1010 (1998).
71 Felley, C., Morris, M. A., Wonkam, A., Hirschel, B., Flepp, M., Wolf, K., Furrer, H., Battegay, M., Bernasconi, E., Telenti, A. & Frossard, J. L. The role of CFTR and SPINK-1 mutations in pancreatic disorders in HIV-positive patients: a case-control study. *AIDS* **18**, 1521-1527, doi:10.1097/01.aids.0000131356.52457.7a (2004).
72 Yadav, D., Nair, S., Norkus, E. P. & Pitchumoni, C. S. Nonspecific hyperamylasemia and hyperlipasemia in diabetic ketoacidosis: incidence and correlation with biochemical abnormalities. *Am J Gastroenterol* **95**, 3123-3128, doi:10.1111/j.1572-0241.2000.03279.x (2000).
73 Hart, P. A. & Conwell, D. L. Chronic Pancreatitis: Managing a Difficult Disease. *Am J Gastroenterol* **115**, 49-55, doi:10.14309/ajg.0000000000000421 (2020).
74 Jalal, M., Campbell, J. A. & Hopper, A. D. Practical guide to the management of chronic pancreatitis. *Frontline Gastroenterol* **10**, 253-260, doi:10.1136/flgastro-2018-101071 (2019).
75 Trout, A. T., Abu-El-Haija, M., Anupindi, S. A., Marine, M. B., Murati, M., Phelps, A. S., Rees, M. A., Squires, J. H., Ellery, K. M., Gariepy, C. E., Maqbool, A., McFerron, B. A., Perito, E. R., Schwarzenberg, S. J., Zhang, B., Andersen, D. K., Lowe, M. E., Uc, A., Consortium for the Study of Chronic Pancreatitis, D. & Pancreatic, C. Interobserver Agreement for CT and MRI Findings of Chronic Pancreatitis in Children: A Multicenter Ancillary Study Under the INSPPIRE Consortium. *AJR Am J Roentgenol* **219**, 303-313, doi:10.2214/AJR.21.27234 (2022).
76 Cruz-Monserrate, Z., Gumpper, K., Pita, V., Hart, P. A., Forsmark, C., Whitcomb, D. C., Yadav, D., Waldron, R. T., Pandol, S., Steen, H., Anani, V., Kanwar, N., Vege, S. S., Appana, S., Li, L., Serrano, J., Rinaudo, J. A. S., Topazian, M., Conwell, D. L., Consortium for the Study of Chronic Pancreatitis, D. & Pancreatic, C. Biomarkers of Chronic Pancreatitis: A systematic literature review. *Pancreatology* **21**, 323-333, doi:10.1016/j.pan.2021.01.006 (2021).
77 Wine, J. J., Hansson, G. C., Konig, P., Joo, N. S., Ermund, A. & Pieper, M. Progress in understanding mucus abnormalities in cystic fibrosis airways. *J Cyst Fibros* **17**, S35-S39, doi:10.1016/j.jcf.2017.09.003 (2018).
78 Hoegger, M. J., Fischer, A. J., McMenimen, J. D., Ostedgaard, L. S., Tucker, A. J., Awadalla, M. A., Moninger, T. O., Michalski, A. S., Hoffman, E. A., Zabner, J., Stoltz, D. A. & Welsh, M. J. Impaired mucus detachment disrupts mucociliary transport in a piglet model of cystic fibrosis. *Science* **345**, 818-822, doi:10.1126/science.1255825 (2014).

79 Carraro, G., Langerman, J., Sabri, S., Lorenzana, Z., Purkayastha, A., Zhang, G., Konda, B., Aros, C. J., Calvert, B. A., Szymaniak, A., Wilson, E., Mulligan, M., Bhatt, P., Lu, J., Vijayaraj, P., Yao, C., Shia, D. W., Lund, A. J., Israely, E., Rickabaugh, T. M., Ernst, J., Mense, M., Randell, S. H., Vladar, E. K., Ryan, A. L., Plath, K., Mahoney, J. E., Stripp, B. R. & Gomperts, B. N. Transcriptional analysis of cystic fibrosis airways at single-cell resolution reveals altered epithelial cell states and composition. *Nat Med* **27**, 806-814, doi:10.1038/s41591-021-01332-7 (2021).

80 Simeone, D. M., Ji, B., Banerjee, M., Arumugam, T., Li, D., Anderson, M. A., Bamberger, A. M., Greenson, J., Brand, R. E., Ramachandran, V. & Logsdon, C. D. CEACAM1, a novel serum biomarker for pancreatic cancer. *Pancreas* **34**, 436-443, doi:10.1097/MPA.0b013e3180333ae3 (2007).

81 Nagaishi, T., Chen, Z., Chen, L., Iijima, H., Nakajima, A. & Blumberg, R. S. CEACAM1 and the regulation of mucosal inflammation. *Mucosal Immunol* **1 Suppl 1**, S39-42, doi:10.1038/mi.2008.50 (2008).

82 Rius, J., Guma, M., Schachtrup, C., Akassoglou, K., Zinkernagel, A. S., Nizet, V., Johnson, R. S., Haddad, G. G. & Karin, M. NF-kappaB links innate immunity to the hypoxic response through transcriptional regulation of HIF-1alpha. *Nature* **453**, 807-811, doi:10.1038/nature06905 (2008).

83 Chen, X., Ji, B., Han, B., Ernst, S. A., Simeone, D. & Logsdon, C. D. NF-kappaB activation in pancreas induces pancreatic and systemic inflammatory response. *Gastroenterology* **122**, 448-457, doi:10.1053/gast.2002.31060 (2002).

84 Ng, B., Viswanathan, S., Widjaja, A. A., Lim, W. W., Shekeran, S. G., Goh, J. W. T., Tan, J., Kuthubudeen, F., Lim, S. Y., Xie, C., Schafer, S., Adami, E. & Cook, S. A. IL11 Activates Pancreatic Stellate Cells and Causes Pancreatic Inflammation, Fibrosis and Atrophy in a Mouse Model of Pancreatitis. *Int J Mol Sci* **23**, doi:10.3390/ijms23073549 (2022).

85 Dolensek, J., Rupnik, M. S. & Stozer, A. Structural similarities and differences between the human and the mouse pancreas. *Islets* **7**, e1024405, doi:10.1080/19382014.2015.1024405 (2015).

86 Kambhampati, S., Park, W. & Habtezion, A. Pharmacologic therapy for acute pancreatitis. *World J Gastroenterol* **20**, 16868-16880, doi:10.3748/wjg.v20.i45.16868 (2014).